

Lysine-based surfactants in nanovesicle formulations: the role of cationic charge position and hydrophobicity in in vitro cytotoxicity and intracellular delivery

Journal:	<i>Nanotoxicology</i>
Manuscript ID:	Draft
Manuscript Type:	Original Article
Date Submitted by the Author:	n/a
Complete List of Authors:	Nogueira, Daniele; Universitat de Barcelona, Moran, Maria del Carmen; Universitat de Barcelona, Mitjans, Montserrat; Universitat de Barcelona, Perez, Lourdes; IQAC, CSIC, Ramos, David; Parc Cientific de Barcelona, de Lapuente, Joaquin; Parc Cientific de Barcelona, Vinardell, Pilar; Universitat de Barcelona,
Keywords:	Drug Delivery, Nanotoxicology

SCHOLARONE™
Manuscripts

1
2
3 **Lysine-based surfactants in nanovesicle formulations: the role of cationic charge position**
4
5 **and hydrophobicity in *in vitro* cytotoxicity and intracellular delivery**
6
7
8
9

10
11 Daniele Rubert Nogueira¹, M. Carmen Morán^{1,4}, Montserrat Mitjans^{1,4}, Lourdes Pérez², David
12 Ramos³, Joaquín de Lapuente³, M. Pilar Vinardell^{1,4,*}
13
14
15

16
17
18
19
20 ¹*Departament de Fisiologia, Facultat de Farmàcia, Universitat de Barcelona, Av. Joan XXIII*
21 *s/n, 08028, Barcelona, Spain*
22

23
24
25 ²*Departamento de Tecnología Química y de Tensioactivos, IQAC, CSIC, C/Jordi Girona 18-26,*
26 *08034, Barcelona, Spain*
27

28
29 ³*Unidad de Toxicología y Ecotoxicología del Parc Científic de Barcelona, Baldiri Reixac 4,*
30 *08028, Barcelona, Spain*
31

32
33 ⁴*Unidad Asociada al CSIC, Spain*
34
35
36
37
38
39

40 * Corresponding author

41
42 Tel: (+34) 934024505; Fax: (+34) 934035901

43
44
45 *E-mail: mpvinardellmh@ub.edu (M. Pilar Vinardell)*
46
47
48
49

50 **Keywords:** nanotoxicity, pH-sensitivity, drug delivery, cell culture, cell internalization.
51
52
53
54
55
56
57
58
59
60

ABSTRACT

Understanding nanomaterial interactions within cells is of increasing importance for assessing their toxicity and cellular transport. Here, we developed nanovesicles containing bioactive cationic lysine-based amphiphiles, and assessed whether these cationic compounds increase the likelihood of intracellular delivery and modulate toxicity. We found different cytotoxic responses among the formulations, depending on surfactant, cell line and endpoint assayed. The induction of mitochondrial dysfunction, oxidative stress and apoptosis were the general mechanisms underlying cytotoxicity. Fluorescence microscopy analysis demonstrated that nanovesicles were internalized by HeLa cells, and evidenced that their ability to release endocytosed materials into cell cytoplasm depends on the structural parameters of amphiphiles. The cationic charge position and hydrophobicity of surfactants determine the nanovesicle interactions within the cell and, thus, the resulting toxicity and intracellular behavior after cell uptake of the nanomaterial. The insights into some toxicity mechanisms of these new nanomaterials contribute to reducing the uncertainty surrounding their potential health hazards.

Introduction

Nanomaterials (NMs) are classically defined as substances that have one or more external dimensions on a sub-100 nm scale (Horie et al. 2012), although some authors classify them as all submicronic particles up to 200 nm (Paillard et al. 2010). At this size, NMs might be easily taken up by cells and interact in a unique fashion with biological systems, which opens up a wide range of interesting applications, including the development of drug and gene delivery systems (Robbens et al. 2010).

Lipid bilayer vesicles are the most prominent colloidal drug carriers, as they can transport drug molecules into the interior of the vesicle, solubilize drugs in the lipid bilayer, or adsorb drugs at the lipid-water interface (Cevc 2012; Liang and Chou 2009). To date, all pharmaceutically used lipid-based vesicles consist of phospholipids (mainly phosphatidylcholine) supplemented with cholesterol, due to the widespread, but not always justified, belief that this is a prerequisite for bilayer stability (Cevc 2012). The inclusion of additives in lipid-based vesicles might help to fulfill the unmet, or partially unmet, goals of these lipid delivery systems. For example, it may increase absorption, improve controlled release and target specificity (Bombelli et al. 2005), and facilitate intracellular delivery (Chen et al. 2004). Additives with non-viral properties, including surfactants, lipids, peptides and polymers, are being intensively studied (Chen et al. 2004; Liang and Chou 2009; Zhang et al. 2004). In this line of research, current directions and the reported advantageous features of the amino acid-based surfactants (Colomer et al. 2012; Nogueira et al. 2011a, 2012a; Pérez et al. 2009) make them a promising group of novel additives for this kind of drug carriers (Lundberg et al. 2011; Morán et al. 2010). The amino acid-based amphiphiles have a structural relationship with endogenous substances and their synthesis can largely be based on non-toxic building blocks, which potentially gives them good biocompatibility (Infante et al. 2010; Lundberg et al. 2011).

1
2
3 Advances in strategies for treating a wide variety of diseases require the efficient
4 delivery of active compounds into the cytosol of target cells (Hu et al. 2007). One common
5 strategy for the intracellular delivery of encapsulated and/or intercalated material *via* lipid-based
6 vesicles exploits intracellular pH gradients (Pollock et al. 2010). Therefore, an approach for
7 cytosolic drug delivery is the development of pH-sensitive lipid-based vesicles (Di Marzio et al.
8 2011; Simões et al. 2004), which contain pH-responsive components that are stable at
9 physiological pH (7.4), but undergo destabilization under the acidic environments encountered
10 during endocytosis. Consequently, their contents are released at intracellular level (Di Marzio et
11 al. 2011). In our previous studies on amino acid-based surfactants, we showed that new cationic
12 lysine-based amphiphiles (hydrochloride salts of N^e-acyl lysine methyl ester) have pH-
13 responsive membrane lytic activity (Nogueira et al. 2012a, 2012b). Thus, they are highly
14 suitable for incorporation in carriers designed for intracellular drug delivery. The potential
15 advantages of this class of cationic lysine-based surfactants as additives in devices designed for
16 drug delivery motivated us to develop new nanovesicles (NVs) containing these amphiphiles as
17 surface modification agents. We study whether these cationic compounds increase the likelihood
18 of intracellular delivery, establish the physicochemical properties of such carriers and modulate
19 their cytotoxic potential. In line with the likely advantages of cationic delivery systems, cationic
20 lipid-based carriers have attracted considerable interest because of their use as effective drug
21 and gene delivery systems (Dakwar et al. 2012; Lundberg et al. 2011; Ramezani et al. 2009).

22
23
24
25
26
27
28
29
30
31
32
33
34
35
36
37
38
39
40
41
42
43
44
45 In the present study, we assessed the impact of including three cationic lysine-based
46 surfactants in lipid-based NVs. These amphiphiles differed in the cationic charge position and
47 the alkyl chain length. Consequently, we investigated specifically whether these structural
48 parameter changes play a key role in the general outcome of the NVs. The potential topical
49 application of these formulations were explored in our previous study, in which we showed no
50 phototoxicity, slight inflammatory potential, and acceptable toxic responses in representative
51
52
53
54
55
56
57
58
59
60

1
2
3 skin cell lines (Nogueira et al. 2013). Here, we tested the feasibility of these NVs as efficient
4
5 drug delivery devices for intravenous administration and intracellular delivery of biomolecules.
6
7 With this objective, we focused on the performance of a broad *in vitro* nanotoxicity study of
8
9 these new nanocarriers, together with an assessment of their uptake by cells and ability to
10
11 deliver contents intracellularly, using Nile red and calcein as fluorescent markers, respectively.
12
13 We aimed to increase understanding of the various steps in nanocarrier cytotoxicity, as little is
14
15 known about the mechanisms underlying this effect. The potential toxic mechanisms of the
16
17 increasing number of nanocarriers have not been explained sufficiently. Additionally,
18
19 relationships between the cytotoxic responses and NM composition are not well understood.
20
21 Thus, the search for reliable conditions to assess NM safety is an emerging field that poses many
22
23 interesting challenges (Marquis et al. 2009).
24
25
26
27
28

29 **Materials and Methods**

30 **Chemicals and reagents**

31
32 Acridine orange (AO), ethidium bromide (EB), propidium iodide, ribonuclease A (RNase A),
33
34 Nile red (NR), calcein, 2,5-diphenyl-3-(4,5-dimethyl-2-thiazolyl) tetrazolium bromide (MTT),
35
36 neutral red (NR) dye, 4,6-diamidino-2-phenylindole dihydrochloride (DAPI), 1,2-dimyristoyl-
37
38 sn-glycero-3-phosphocholine (DMPC), cholesterol (CHOL) and dimethylsulphoxide (DMSO)
39
40 were obtained from Sigma-Aldrich (St. Louis, MO, USA). Dulbecco's Modified Eagle's
41
42 Medium (DMEM), fetal bovine serum (FBS), phosphate buffered saline (PBS), L-glutamine
43
44 solution (200 mM), trypsin-EDTA solution (170,000 U/l trypsin and 0.2 g/l EDTA) and
45
46 penicillin-streptomycin solution (10,000 U/ml penicillin and 10 mg/ml streptomycin) were
47
48 purchased from Lonza (Verviers, Belgium). The 75 cm² flasks and 96-well plates were obtained
49
50 from TPP (Trasadingen, Switzerland). All other reagents were of analytical grade.
51
52
53
54
55
56

57 **Surfactants included in the nanovesicular systems**

1
2
3 Three new biocompatible amino acid-based surfactants with one lysine as the cationic polar
4 head (one cationic charge) and one alkyl chain were used as surface modification agents to
5 prepare the cationic nanovesicular systems reported in this study. The surfactants were: N^ε-
6 myristoyl lysine methyl ester (MKM) with one alkyl chain of 14 carbon atoms and one positive
7 charge on the α-amino group of the lysine; N^ε-palmitoyl lysine methyl ester (PKM) with one
8 alkyl chain of 16 carbon atoms and one positive charge on the α-amino group of the lysine; and
9 N^α-myristoyl lysine methyl ester (MLM) with one alkyl chain of 14 carbon atoms and one
10 positive charge on the ε-amino group of the lysine. MKM and PKM have a hydrophobic chain
11 attached to the ε-amino group of the lysine, while MLM has its hydrophobic chain attached to
12 the α-amino group. These lysine-based surfactants were synthesized in our laboratory, as
13 described elsewhere (Colomer et al. 2012; Pérez et al. 2009).
14
15
16
17
18
19
20
21
22
23
24
25
26
27

28 **Preparation of cationic nanovesicular formulations**

29
30 The mixed cationic NVs were prepared by the film hydration method, as previously described
31 (Nogueira et al. 2013). DMPC and cholesterol (CHOL) were selected as basic lipid membrane
32 components and were mixed with MKM, PKM or MLM in the designed molar ratios, as
33 described in the Table 1. The total final concentration of each mixed cationic NV was fixed at 2
34 mM. NV dispersions were purified by filtration using Vivaspin 2 centrifugal concentrator (PES
35 membrane, 3,000 MWCO, Sartorius Stedim Biotech, Goettingen, Germany). The filtered
36 substance was used to determine the extent of incorporation of the cationic surfactants into the
37 vesicles and the amount of unincorporated surfactant was assessed by high-performance liquid
38 chromatography, following the previously described analytical method (Pérez et al. 2009).
39
40
41
42
43
44
45
46
47
48
49

50 NVs physically encapsulating Nile red as a fluorescent marker (NR-NVs) were also
51 prepared. The formulation DMPC:MKM (80:20, w/w) was used as a model in this study. Nile
52 red 1 mol% (of the final concentration of the formulation), was dissolved with the phospholipid
53 and the surfactant prior to obtaining the film. Then, the nanovesicle preparation followed the
54
55
56
57
58
59
60

1
2
3 same procedure as that described above. The NR-NVs were further purified to eliminate the
4
5 non-encapsulated dye by ultracentrifugation with multiple washing with ultrapure water.
6
7

8 **Nanovesicle characterization**

9
10 The mean hydrodynamic diameter and the polydispersity index (PDI) of the cationic NVs were
11
12 determined by dynamic light scattering (DLS) using a Malvern Zetasizer ZS (Malvern
13
14 Instruments, Malvern, UK). Before measurement, the NVs were appropriately diluted in
15
16 ultrapure water or cell culture medium with 5% (v/v) FBS. Readings were taken at 25°C
17
18 immediately after preparation (t = 0 h) and after a 24 h incubation at 37°C (t = 24 h). Each
19
20 measurement was performed using at least three sets of a minimum of ten runs. The zeta
21
22 potential (ZP) values of the NVs were assessed by determining electrophoretic mobility with the
23
24 Malvern Zetasizer ZS equipment. The measurements were also performed in ultrapure water and
25
26 cell culture medium with 5% (v/v) FBS (t = 0 h, 25°C), using at least three sets of a minimum of
27
28 20 runs. These experiments were performed as previously described (Nogueira et al. 2013), but
29
30 additional analyses were carried out to assess the NV stability in ultrapure water after 24 h and 1
31
32 week incubation at 37°C and 4°C, respectively.
33
34
35
36

37 The morphology and size of the NVs were analyzed by transmission electron microscopy
38
39 (TEM), as previously described (Nogueira et al. 2013). The images were obtained with a Jeol
40
41 JEM-1010 electron microscope (Jeol Ltd., Tokyo, Japan) operating at an acceleration voltage of
42
43 80 kV.
44
45
46

47 **Cell cultures**

48
49 The 3T3 (murine Swiss albino fibroblasts) and the HeLa (human epithelial cervical cancer) cell
50
51 lines were grown in DMEM medium (4.5 g/l glucose) supplemented by 10% (v/v) FBS, 2 mM
52
53 L-glutamine, 100 U/ml penicillin and 100 µg/ml streptomycin at 37°C, 5% CO₂. These cells
54
55 were routinely cultured in 75 cm² culture flasks and were trypsinized using trypsin-EDTA when
56
57
58
59
60

1
2
3 the cells reached approximately 80% confluence. The cell lines were obtained from Eucellbank
4 (Universitat de Barcelona, Spain). We selected these cell lines as model systems because the use
5 of cells from different species and with different embryonic origins is an important approach to
6 understand the cell specific responses induced by NMs (Fröhlich et al. 2012).
7
8
9

10 11 12 **Cytotoxicity assays: MTT, NRU and LDH**

13 The 3T3 (1×10^5 cells/ml) and HeLa (5×10^4 cells/ml) cells were seeded into the 60 central
14 wells of 96-well cell culture plates in 100 μ l of complete culture medium. Cells were incubated
15 for 24 h under 5% CO₂ at 37°C. The medium was then replaced with 100 μ l of fresh medium
16 supplemented by 5% (v/v) FBS containing the NV dispersions in the 0.5 – 100 μ M
17 concentration range. The surfactants only and NVs without any surfactant (DMPC only and
18 DMPC:CHOL 70:30) were also assessed in the same concentration range. Each concentration
19 was tested in triplicate and control cells were exposed to the medium with 5% (v/v) FBS only.
20 The cell lines were incubated for 24 h with each treatment.
21
22
23
24
25
26
27
28
29
30
31

32 The MTT assay is a measurement of cell metabolic activity in the mitochondria of viable
33 cells and was performed as previously described (Nogueira et al. 2013). Cell viability was
34 calculated as the percentage of tetrazolium salt reduction by viable cells in each sample and the
35 values were normalized by the untreated cell control (cells with medium only).
36
37
38
39
40
41

42 The NRU assay determines the accumulation of NR dye in the lysosomes of cells and
43 reflects the functionality of the lysosomes and plasma membrane (Fröhlich et al. 2012). The
44 assay was performed following the previously described methodology (Nogueira et al. 2013).
45 The effect of each treatment was calculated as the percentage of uptake of NR dye by lysosomes
46 against the untreated cell control (cells with medium only).
47
48
49
50
51

52 LDH leakage was determined in the conditioned medium using a commercially available
53 kit (Takara Bio Inc, Otsu, Japan), according to the instructions provided by the manufacturer.
54 This assay is an indicator of plasma membrane integrity and quantifies cytotoxicity by
55
56
57
58
59
60

1
2
3 measuring LDH released from dead or plasma membrane-damaged cells into the supernatant
4
5 (Yang et al. 2009). Results are expressed as a percentage of the control, with 1% (v/v) Triton-X
6
7 used as a positive control.
8

9
10 One of the possible limitations of the cytotoxicity study of NMs is their interference with
11
12 the dyes used in the viability assays. Therefore, we determined whether the NVs interact with
13
14 the viability assays using UV-visible absorbance measurements (Monteiro-Riviere et al. 2009,
15
16 2010). NVs at 100 μM were suspended in DMEM medium (without FBS and phenol red)
17
18 containing MTT (0.5 mg/ml) or NR (50 $\mu\text{g}/\text{ml}$) dyes, and the occurrence of dye interference was
19
20 assessed following the procedure previously described (Nogueira et al. 2013).
21
22

23 24 **Apoptosis**

25
26 NV-induced apoptosis in 3T3 cells was quantified using acridine orange/ethidium bromide
27
28 (AO/EB) double staining, according to standard procedure (Squier and Cohen 2001). Samples
29
30 were examined under a fluorescence microscope. Briefly, cells were seeded (1×10^5 cells/ml) in
31
32 24-well plates and treated with IC_{50} concentration (calculated by MTT assay). After 24 h
33
34 incubation, the cells were trypsinized and centrifuged at 1200 rpm for 5 min. Then, the
35
36 fluorescent dyes AO (0.5 $\mu\text{g}/\text{ml}$) and BE (10 $\mu\text{g}/\text{ml}$) were added to the cellular pellet. The
37
38 freshly stained cell suspension was dropped on a glass slide and covered by a cover slip. Slides
39
40 were observed under a fluorescent microscope (Olympus BX41 microscope equipped with a
41
42 UV-mercury lamp, 100W Ushio Olympus, and a filter set type MNIBA3 470-495 nm excitation
43
44 and 505 nm dichromatic mirror) and the percentage of viable, apoptotic, late apoptotic and
45
46 necrotic cells was determined in at least 100 cells.
47
48
49
50

51 52 **Cell cycle analysis by flow cytometry**

53
54 The 3T3 fibroblasts were cultured in 60 mm petridishes for 24 h at a density of 1×10^5 cells/ml
55
56 and then treated with IC_{20} and IC_{50} concentrations of each NV formulation. After 24 h treatment,
57
58
59
60

1
2
3 the cells were harvested by trypsinization, washed in cold PBS, fixed in ice-cold 70% ethanol
4
5 and kept at -20°C. Fixed cells were centrifuged, resuspended in DNA extraction buffer (0.2 M
6
7 Na₂PO₄ and 0.1 M citric acid, pH 7.8) and incubated for 30 min at 37°C. Then, the cells were
8
9 centrifuged and stained with staining solution (20 µg/ml propidium iodide, 200 µg/ml RNase A
10
11 and Triton X-100 in PBS). The samples were kept in dark conditions for 1 h and measured with
12
13 the Beckman Coulter ADC Epics XL flow cytometer (Beckman Coulter, FL, USA). The amount
14
15 of propidium iodide intercalating to DNA was used as the parameter to determine the cell cycle
16
17 distribution phases. Aggregates were excluded gating single cells by their area vs. peak
18
19 fluorescence signal. DNA analysis on single fluorescence histograms was done using Multicycle
20
21 software (Phoenix Flow Systems, CA, USA).
22
23
24

25 26 **Genotoxicity**

27
28 DNA damage in the form of unrepaired single- and double-strand DNA breaks was detected
29
30 using an alkaline single cell gel electrophoresis/comet assay, according to the method described
31
32 by Singh et al. (1988), with some modifications by Di Guglielmo et al. (2012). The 3T3 cells
33
34 were treated with the IC₁₀, IC₂₀ and IC₃₀ concentrations (calculated by MTT assay) of each NV
35
36 formulation. After 24 h incubation, the cells from 2 wells of each treatment were trypsinized and
37
38 transferred to eppendorfs. Slides containing the samples were prepared. The cells were lysated
39
40 and then incubated in alkaline electrophoresis buffer for DNA unwinding and conversion of
41
42 alkali-labile sites to single-strand breaks. Electrophoresis was performed in the same buffer for
43
44 30 minutes at 25 V and 300 mA. After that, 20 µL of 5 µg/ml DAPI solution was added to each
45
46 slide for the fluorescence microscopy analysis. The migration of nuclear DNA from the cells
47
48 was measured using the COMET ASSAY IV[®] Program (Perspective Instruments) for 50
49
50 randomly selected cell images, and the mean percentage of DNA in the tail (% Tail DNA) was
51
52 calculated in each trial. Methyl methanesulfonate (MMS) at a concentration of 400 µM was used
53
54 as the positive control.
55
56
57
58
59
60

Oxidative damage

Oxidative stress can be determined by biomarker stress products from lipid peroxidation (Marquis et al. 2009). We employed the reaction of malondialdehyde (MDA) with thiobarbituric acid (TBA) to indicate the oxidative damage caused by NVs. MDA is the end product of the peroxidation of polyunsaturated fatty acids, and has been extensively used as an index for lipid peroxidation. The 3T3 fibroblasts were cultured in 60 mm petri dishes for 24 h at a density of 1×10^5 cells/ml and then treated with IC_{50} concentrations of each NV formulation. After 24 h treatment, the cells were trypsinized, centrifuged and resuspended in PBS. For the lipid extraction, cells were incubated with 3.2% SDS and 30% acetic acid, and 0.8% TBA was added. The reaction was carried out at $95^{\circ}C$ for 1 h and the absorbance was then determined at 532 nm using a microplate reader. The MDA concentration in each sample was obtained from an MDA calibration curve (0 - 15 nM/ml). The values were normalized against the total cell protein content and the results expressed as nM MDA/mg protein. The protein content of the cell lysate was determined by a commercial kit (Bio-Rad, CA, USA) based on the Bradford dye-binding procedure (Bradford 1976). Hydrogen peroxide (H_2O_2) at a concentration of 100 μM was included in the assay as a positive control.

Blood compatibility studies

Hemolysis and agglutination assays

Erythrocytes were isolated from rat blood, which was obtained from anesthetized animals by cardiac puncture and drawn into tubes containing EDTA. The procedure was approved by the institutional ethics committee on animal experimentation. The hemolysis assay was performed following the previously described procedure (Nogueira et al. 2011a). Aliquots of 25- μl of erythrocyte suspension were exposed to NV concentrations of 20, 100 and 200 μM , and dissolved in PBS buffer in a total volume of 1 ml. Two controls were prepared by resuspending erythrocyte suspension either in buffer alone (negative control) or in distilled water (positive

1
2
3 control). The samples were incubated at room temperature for 10 minutes or 1 h and then
4
5 centrifuged at 10,000 rpm for 5 min. Absorbance of the hemoglobin release in supernatants was
6
7 measured at 540 nm using a Shimadzu UV-160A spectrophotometer (Shimadzu, Kyoto, Japan)
8
9 and the percentages of hemolysis were determined by comparison with the positive control
10
11 samples completely hemolyzed with distilled water. For the erythrocyte agglutination studies, 10
12
13 μ l of each sample that had been subjected to a hemolysis assay (100 μ M for 1 h) were placed on
14
15 a glass slide, covered by a cover slip and analyzed by a phase contrast microscope (Olympus
16
17 BX41, Olympus, Japan).
18
19

20 21 **Human plasma protein adsorption by SDS-PAGE and total protein assay**

22
23 Blood was drawn from the authors by venipuncture into tubes containing EDTA. It was then
24
25 centrifuged at 3000 rpm to obtain fresh plasma. NVs (200 μ M) were suspended in plasma
26
27 diluted with PBS to 10% of normal strength and incubated for 1 h at 37°C with constant shaking.
28
29 The NVs were separated from the plasma by multiple cycles of ultracentrifugation and washing
30
31 steps with PBS. Firstly, an aliquot of the supernatant of each sample was taken and mixed with
32
33 electrophoresis sample buffer. Then, the proteins adsorbed to the NVs were desorbed by
34
35 sonication in electrophoresis sample buffer for 20 min. Both samples were incubated at 95°C for
36
37 5 min. Thereafter, samples were applied onto pre-cast polyacrylamide gel (7.5% resolving gel
38
39 and a 5% stacking gel). Electrophoresis was carried out for 10 min at 60 V followed by 35 min
40
41 at 200 V. Protein bands were viewed by staining with Coomassie Brilliant Blue R-250 for an
42
43 hour under gentle shaking. Samples were then destained with a mixture of 7.5% methanol and
44
45 10% acetic acid. The molecular weight of the membrane proteins was estimated from the
46
47 molecular size marker (Bio-Rad Precision Plus Unstained Standard), and ranged from 10 to 250
48
49 kDa. Finally, portions of the supernatant and the fluid desorbed from NVs were also taken for
50
51 total protein assay using the Bio-Rad kit (Bio-Rad, CA, USA), which is based on the Bradford
52
53
54
55
56
57
58
59
60

dye-binding procedure (Bradford 1976), using bovine serum albumin (BSA) as a protein standard.

Cell uptake studies

Intracellular localization of Nile red-labeled nanovesicles

To study the cell uptake, DMPC:MKM (80:20, w/w) NVs that physically encapsulated Nile red (NR-NVs) were prepared. HeLa cells were plated in 24-well plates at a density of 5×10^4 cells/ml on round cover glasses (Marlenfeld GmbH & Co.KG, Lauda-Könlghshofen, Germany) and incubated overnight at 37°C under 5% CO₂. After that, the culture medium was replaced with fresh medium containing NR-NVs at a final concentration of 50 μM (0.5 μM of NR) and incubated for 2 h and 24 h. Following incubation, the test samples were aspirated and the cells were washed three times with PBS and fixed with 4% (v/v) formaldehyde in PBS (pH 7.4) for 15 min at room temperature. The individual cover glasses were then mounted on clean glass slides with Prolong® Gold antifade reagent (Invitrogen, OR, USA) for subsequent fluorescence microscopy analysis (Olympus BX41 microscope equipped with a UV-mercury lamp, 100W Ushio Olympus, and a filter set type MNIBA3 470-495 nm excitation and 505 nm dichromatic mirror). Images were digitized on a computer through a video camera (Olympus digital camera XC50) using an image processor (Olympus cell^B Image Acquisition Software). The images were then analyzed with ImageJ software (v. 1.46, National Institutes of Health, MD, USA) (Collins 2007; Rasband 1997) to calculate the mean fluorescence value of the cells, which corresponds to the cell internalization of NVs. For each condition, ~20 individual cells from different fields and images were analyzed and their total fluorescence intensity was quantified.

Intracellular release of calcein

Calcein (a membrane-impermeable fluorophore) was used as a tracer molecule to monitor the effect of the NVs on endosomes after cell internalization. HeLa cells were plated (5×10^4

1
2
3 cells/ml) in 24-well plates on round cover glasses (Marlenfeld GmbH & Co.KG, Lauda-
4
5 Könlghshofen, Germany) and incubated overnight at 37°C under 5% CO₂. Then, calcein (1
6
7 mg/ml) was added to the cells with or without (control cells) 50 µM of each NV formulation in
8
9 DMEM medium without FBS and phenol red. After 1 h incubation at 37°C, the cells were
10
11 washed four times with PBS and incubated in complete medium for 3 h to allow intracellular
12
13 trafficking. The cells were then washed four times with PBS and fixed with 4% (v/v)
14
15 formaldehyde in PBS (pH 7.4) for 15 min at room temperature. Each individual cover glasses
16
17 was mounted on a clean glass slide with Prolong® Gold antifade reagent (Invitrogen, OR, USA)
18
19 and analyzed on a Olympus BX41 fluorescence microscope equipped with a UV-mercury lamp
20
21 (100W Ushio Olympus) and a filter set type MNIBA3 (470-495 nm excitation, 510-550 nm
22
23 emission and 505 nm dichromatic mirror). Images were digitized on a computer through a video
24
25 camera (Olympus digital camera XC50) using an image processor (Olympus cell^B Image
26
27 Acquisition Software). Thereafter, ImageJ software was used to calculate the average pixel
28
29 intensity of calcein fluorescence within regions of interest (ROI) drawn on to collected images.
30
31 Images of ~20 individual cells were analyzed for each treatment. This was done by drawing
32
33 three ROI inside the cell (excluding any calcein-containing vesicles and, thus, representing the
34
35 cytoplasm only) and the results were obtained in arbitrary fluorescence units (Jones et al. 2003).
36
37
38
39
40

41 **Statistical analysis**

42
43 The results of all *in vitro* assays are expressed as mean ± standard error of the mean (SEM) of
44
45 three independent experiments, which were performed using three replicate samples for each
46
47 concentration tested. The cytotoxicity of each formulation was expressed in terms of its IC₅₀ (the
48
49 concentration causing 50% death of the cell population), calculated from concentration-response
50
51 curves. Statistical analyses used the Student's *t* test or the one-way analysis of variance
52
53 (ANOVA) to determine the differences between the datasets, followed by Dunnett's *post-hoc*
54
55
56
57
58
59
60

1
2
3 test for multiple comparisons using SPSS[®] software (SPSS Inc., Chicago, IL, USA). $p < 0.05$
4
5 and $p < 0.005$ were considered significant.
6
7

8 **Results**

9 **Characterization of cationic nanovesicles**

10
11 As was previously reported (Nogueira et al. 2013), we assessed the effects of the dispersion
12 medium (ultrapure water or cell culture medium) on NV hydrodynamic size (Table 2). Here, we
13 have extended the NV characterization and also evaluated the effects of temperature and
14 exposure time on the stability of the formulations in ultrapure water. DLS measurements showed
15 that after 24 h incubation (37°C) in ultrapure water, the NVs showed slightly lower diameters or
16 did not consistently increase in comparison to fresh prepared NVs ($t = 0$), with the exception of
17 the NVs containing PKM, which almost doubled in size. When the NVs were dispersed in cell
18 culture medium (DMEM with 5% [v/v] FBS) the size increase was slight by 0 h, but significant
19 agglomeration to micron-sized structures occurred after 24 h incubation under cell culture
20 conditions (37°C), with the exception of the NVs containing MLM. As observed from the PDI
21 values, the increase in NV polydispersity was slight to moderate after 24 h incubation at 37°C in
22 water. However, in general, substantially higher PDI values were obtained after incubation in
23 cell culture medium. The ZP values of all formulations dispersed in water were highly positive
24 (> 40 mV), whereas almost neutral values were obtained in cell culture medium. The NVs
25 containing MLM showed the most positive ZP values in DMEM medium (~ 10 mV). The
26 purification process with a Vivaspin column resulted in no significant changes in NV size, PDI,
27 or ZP (data not shown). Preservation of the mean hydrodynamic size and zeta potential was
28 observed for at least one week at 4°C, with the exception of the formulation
29 DMPC:CHOL:PKM, proving the generally good physical stability of these colloidal
30 formulations. Finally, the HPLC measurements of the filtered samples (obtained from the
31
32
33
34
35
36
37
38
39
40
41
42
43
44
45
46
47
48
49
50
51
52
53
54
55
56
57
58
59
60

1
2
3 purification process performed to remove the unincorporated amount of surfactant) revealed that
4
5 the cationic surfactants were highly incorporated into the NVs (from 75 to 99% incorporation).
6

7 The TEM analysis (Table 2) showed that the cationic NVs containing MKM and PKM
8
9 were predominantly much smaller (~ 20 – 50 nm) than the hydrodynamic size determined by
10
11 DLS (~ 100 or 200 nm, respectively). These differences were especially significant for the NVs
12
13 with MKM, while the formulations with PKM showed a more heterogeneous size distribution (2
14
15 predominant populations: 20 – 50 nm and 100 – 150 nm). In contrast, TEM images corroborated
16
17 the mean hydrodynamic size obtained by DLS for the NVs containing MLM. Moreover, the
18
19 TEM images revealed the formation of a multilayered membrane in the NVs containing MLM,
20
21 while those containing MKM and PKM showed unilamellar membranes in both the presence
22
23 and absence of cholesterol in the basic membrane.
24
25
26
27

28 **Cytotoxicity assays**

29 **Cell viability studies**

30
31 The cytotoxicity of each surfactant in its free form was firstly assessed in 3T3 cell line (Figure
32
33 1a), in which it was observed a greater reduction of the cell viability in comparison to the
34
35 correspond formulations. Thereafter, the NV effects on the viability of 3T3 (Nogueira et al.
36
37 2013) and HeLa cells were evaluated by three different endpoints (MTT, NRU and LDH).
38
39 Indeed, the cytotoxic effects of NVs showed many disparities between formulations that, in fact,
40
41 depended on the surfactant, cell line and endpoint assayed. These disparities can be seen in the
42
43 dose-response curves illustrated in Figure 1. The NVs containing MKM and PKM induced a
44
45 clear dose-dependent decrease in MTT activity (Figures 1b,c). In contrast, the NRU assay
46
47 showed markedly low cytotoxicity with a significant decline in cell viability only at the highest
48
49 doses assessed (> 50 μ M) (Figures 1d,e). In the same way, the LDH release results only showed
50
51 significant cytotoxicity at 50 and 100 μ M in 3T3 cells, and to a lesser extent in HeLa cells
52
53 (Figures 1 f,g). NVs containing MLM showed relatively similar cytotoxic responses in the three
54
55
56
57
58
59
60

1
2
3 endpoint assays. The NVs that formed agglomerates after 24 h incubation in cell culture medium
4
5 (those containing MKM and PKM) induced more marked cytotoxic effects to the mitochondria
6
7 (as shown by the MTT assay) than well-dispersed NVs (those containing MLM). NVs without
8
9 any surfactant were also tested as a control of each formulation type and, as expected, it was
10
11 observed that they induced negligible cytotoxic effects (Figures 1b-g). Finally, the NVs
12
13 containing cholesterol were less cytotoxic to both cell lines, which might be related to the low
14
15 surfactant incorporation into these formulations (Table 2). Finally, in studies of MTT and NR
16
17 dye interactions with NVs, we observed only minimal interference of the NVs with the MTT
18
19 dye and no interaction with the NR dye. The formulations induced only a slight increase in the
20
21 MTT absorbance values at 550 nm. These data were proved by the UV-vis measurements (data
22
23 not shown).
24
25
26
27

28 **Apoptosis**

29
30 To assess the extent and mode of cell death, AO/EB staining was carried out and the samples
31
32 analyzed under a fluorescence microscope. The data from this experiment revealed that the NV
33
34 treatment (IC_{50} concentrations) increased the number of cells undergoing apoptosis and necrosis
35
36 (Figure 2a). The most significant effects were observed with the NVs containing PKM, which
37
38 were also the most cytotoxic in all the viability assays. The untreated cells were observed with a
39
40 green intact nuclear structure (Figure 2b), while after NV treatment we observed cells showing
41
42 chromatin condensation (Figure 2c), blebbing and nuclear margination (early and moderate
43
44 apoptosis) (Figures 2d,e), together with cells showing apoptotic body separation and a reddish-
45
46 orange color (late apoptosis) (Figure 2e) and orange nuclei with normal chromatin distribution
47
48 (necrosis) (Figure 2c).
49
50
51
52
53
54
55
56
57
58
59
60

Cell cycle analysis

In addition to the cell viability studies, flow cytometric analysis was performed to clarify the influence of each NV formulation on the cell-cycle distribution. The treatment of 3T3 cells with the IC₂₀ and IC₅₀ concentrations of NVs revealed no significant induction of cell cycle arrest, and only small significant changes were observed in the percentages of cells in each cell phase (Figure 3). Even the most cytotoxic NVs (those containing PKM) showed only a maximal increase in the percentage of cells in the G2/M phase from 15.15% (control) to 20.95%, and a decrease in G1 and S phases from 50.19 and 32.31% (control) to 46.71 and 27.60%, respectively. Moreover, no significant cell population was observed in the sub-G1 phase, which could be attributed to the low proportion of apoptotic cells in relation to the total cell count.

Genotoxicity

DNA damage was further studied using a comet assay, by measuring the % Tail DNA in the control and treated cells. A comet-like tail implies the presence of a damaged DNA strand, and the length of the tail increases with the extent of the DNA damage (Figures 4a-c). The tested concentrations (IC₁₀, IC₂₀ and IC₃₀) of the NVs containing PKM and MLM induced significantly ($p < 0.005$) higher DNA damage than the negative control (Figure 4d). However, these significant responses were ~ 4- to 20-fold lower than that induced by the positive MMS control. No clear dose-dependent response was observed among the three concentrations assessed.

Oxidative damage

MDA concentrations were measured to elucidate the lipid peroxidation induced by NVs. The NVs containing the amphiphiles MKM and PKM statistically ($p < 0.05$) elevated the intracellular MDA level after 24 h exposure, while no significant ($p > 0.05$) response was induced by the formulations containing MLM (Figure 5). The inclusion of cholesterol in the NV formulations resulted in lower MDA generation. Enhanced responses were observed as the

1
2
3 concentration increased (from IC₅₀ MTT to IC₅₀ NRU), with the exception of the formulation
4 DMPC:CHOL:PKM. This failure in dose-dependent response might be directly attributed to the
5 cell death. The NVs DMPC:MKM (IC₅₀ NRU) and DMPC:PKM (IC₅₀ MTT and NRU) showed
6
7 the most prominent responses, as they elevated intracellular MDA to concentrations higher than
8
9 that induced by the positive H₂O₂ control.
10
11
12

13 14 15 **Blood compatibility studies**

16
17 The hemocompatibility of the cationic NVs was studied by hemolysis experiments. The release
18 of hemoglobin was used to quantify the erythrocyte-damaging properties of the NVs. The
19 hemolytic activity of the NVs, with concentrations up to 200 μM, was negligible (less than 5%)
20 after 10 min incubation (data not shown). When the hemolysis assay was performed for 1 h
21 (Figure 6a), the formulations containing MKM showed increased hemolysis at 100 μM, while
22 the NVs containing PKM only prompted enhanced hemolysis at 200 μM. NVs containing MLM
23 did not increase the hemolytic activity at any concentration assayed. Moreover, the NVs
24 containing MKM and MLM did not induce agglutination of erythrocytes after 1 h of treatment
25 (Figures 6b-h), whereas a slight tendency to agglutinate was noticed with the NVs containing
26 PKM (Figures 6e,f).
27
28
29
30
31
32
33
34
35
36
37
38

39 The plasma proteins adsorbed to the NVs were firstly evaluated by SDS-PAGE. In brief,
40 we analyzed the plasma protein present in the supernatant after incubation with NVs. Figure 6i
41 shows the protein banding patterns that appeared after electrophoresis. No qualitative
42 differences were observed in any protein band in comparison to the control plasma sample,
43 which indicates that a negligible or very small amount of plasma protein was adsorbed onto the
44 NVs following incubation under *in vitro* conditions. To further examine the plasma protein
45 adsorption, we assessed the proteins desorbed from the NVs surface, obtained from washed
46 particle pellets. The gel of the proteins adsorbed to NVs from 10% plasma is shown in Figure 6j.
47
48
49
50
51
52
53
54
55
56
57
58
59
60 The lane corresponding to the final wash fluid shows essentially no protein, which confirms that

1
2
3 the wash protocol reduced unbound protein to an insignificant level. No substantial amount of
4
5 protein was associated with the NVs after plasma contact, which indicates the lack of
6
7 nonspecific adsorption. We only observed quite a faint band in the 50 – 75 kDa range of the gel,
8
9 which corresponds to albumin (67 kDa), the most abundant plasma protein. Moreover, it seems
10
11 that the albumin adsorption was higher in the formulations containing cholesterol (Figures 6j,
12
13 lanes 2, 4 and 6). Finally, quantitative analyses of total protein adsorption were performed using
14
15 the BioRad assay. In agreement with the qualitative data obtained from the SDS-PAGE gels, no
16
17 significant differences were observed in the amount of protein in the control plasma and NV-
18
19 treated plasma (data not shown).
20
21
22
23

24 **Cell uptake studies and pH-dependent membrane-lytic activity of NVs**

25
26 The cell uptake of fluorescent-labelled NR-NVs by the HeLa cell line was visualized by a
27
28 fluorescence microscope after 2 h and 24 h incubation (Figure 7A). Fluorescent punctate spots
29
30 were observed mainly in the cell cytosol, which indicates that the NVs were taken up by the
31
32 cells. Moreover, a smaller number of fluorescent spots were detected along the cell membrane,
33
34 but not in the nucleus. Interestingly, 24 h of incubation resulted in a more intensive dotted
35
36 pattern of fluorescent NVs inside the cell, together with some diffuse fluorescence in the
37
38 cytosol. The quantitative analysis of the images corroborated the greater localization of the NVs
39
40 in the intracellular compartments after 24 h of incubation (Figure 7C). The cell uptake was ~ 2-
41
42 fold higher than after 2 h of incubation ($p < 0.005$).
43
44
45

46 The ability of NVs to release endocytosed materials into cell cytoplasm was examined by
47
48 fluorescence microscopy following uptake of calcein and NVs into HeLa cells (Figure 7B).
49
50 Cells treated with calcein alone (control cells) showed a punctuate distribution of fluorescence,
51
52 which is consistent with constitutive endocytosis of the external medium. Moreover, the co-
53
54 incubation of calcein and NVs containing MLM only induced a low release of calcein from
55
56 endosomal compartments. Almost all of the membrane-impermeable fluorophore was restricted
57
58
59
60

1
2
3 within intracellular vesicles appearing as bright punctate structures in a similar level of the
4 control cells. In contrast, when the cells were co-incubated with calcein and NVs containing
5 MKM or PKM, green diffuse fluorescence staining was observed in the cytoplasm, which
6 indicates that calcein had been released from the endosomes. Stronger diffuse staining in the
7 cytoplasm was observed after cell treatment with the NVs containing MKM, whilst a larger
8 number of bright intact vesicles still existed after cell treatment with the NVs containing PKM.
9 Figure 7D shows the quantitative analyses of the cytosolic calcein distribution, which
10 corroborate that the NVs containing MKM or PKM induced significant endosomal
11 destabilization and calcein release ($p < 0.005$), whereas those containing MLM prompted low or
12 negligible membrane-lytic activity at the endosomal compartments ($p < 0.05$ for DMPC:MLM
13 and $p > 0.05$ for DMPC:CHOL:MLM). The presence of cholesterol confers to each formulation
14 a low ability to lysis the endosomal membrane, which can be attributed to the low incorporation
15 of the surfactants into the NV lipid-based structure.

32 Discussion

33
34
35 Chemical composition of the NMs is one of the most important factors influencing cellular
36 interaction. Therefore, the role of including cationic amphiphiles in lipid-based NVs was
37 investigated. We hypothesised that these compounds influences not only the cytotoxic effects,
38 but also the physicochemical properties and intracellular behavior after cell uptake. In order to
39 corroborate this hypothesis, we prepared six different NVs formulations containing three lysine-
40 based surfactants that differ in the cationic charge position and hydrophobicity.

41
42
43
44
45
46
47
48
49 NV hydrodynamic size characterization in cell culture medium suggested significant
50 agglomeration, especially for formulations containing MKM and PKM (positive charge on the
51 α -amino group of lysine). These amphiphiles have pKa values of 5.3 and 4.5 (Nogueira et al.
52 2012a), respectively, which means that at physiological conditions they predominantly exist as
53 unprotonated species and, therefore, the resulting NVs tend to aggregate. The tendency of NMs
54
55
56
57
58
59
60

1
2
3 to agglomerate in cell culture medium during an *in vitro* toxicity assessment has been previously
4 reported (Horie et al. 2012; Monteiro-Riviere et al. 2009, 2010). The easy aggregation or
5 agglomeration in cell culture medium is probably attributed to the high ionic nature of the
6 solution and the electrostatic/van der Waals interaction between protein and NMs, which result
7 in the formation of secondary particles (Horie et al. 2012). In contrast, NVs containing MLM
8 (positive charge on the ϵ -amino group of lysine) were not agglomerated in the cell culture
9 medium. This may be due to their higher charge density at physiological pH (pKa MLM = 8.1),
10 corroborated by the ZP values determined in the cell culture medium. A high charge density
11 increases the physical stability of colloidal dispersions (Liang et al. 2009). These overall
12 findings showed that the cationic charge position in the amphiphile determines the aggregation
13 state of NVs. The high positive ZP values of the NVs in water indicated the stability of the
14 prepared formulations by preventing fusion or aggregation of NVs (Liang et al. 2009). A
15 physically stable formulation would have a minimum ± 30 mV ZP as a borderline value of
16 colloidal stability (Di Marzio et al. 2011; Müller et al. 2011). Interestingly, the mean
17 hydrodynamic diameters measured by DLS did not capture the real size distribution of the NVs
18 observed by TEM. DLS measurements of NVs containing MKM and PKM were larger than
19 those determined from the TEM images of the corresponding samples. Disparity between DLS
20 and TEM might be a result of the resolution limitations of DLS (Coldren et al. 2003; Ojogun et
21 al. 2009), aggregation (Ahmad et al. 2012; Bai et al. 2009; Venkatesan et al. 2011) and swelling
22 of the NVs in the presence of water (Mehrotra et al. 2011), or even to the fact that DLS gives the
23 mean hydrodynamic diameter of the particle core surrounded by the solvation layers, whereas
24 TEM gives the diameter of particles alone in the dry state (Gao et al. 2010).

25
26
27
28
29
30
31
32
33
34
35
36
37
38
39
40
41
42
43
44
45
46
47
48
49
50
51
52 High throughput cell-based tests have been the initial step in biological screening
53 approaches (Monteiro-Riviere et al. 2009). Moreover, *in vitro* cell culture-based cytotoxicity
54 screening assays, designed to minimize animal use in toxicity testing, have become and are
55
56
57
58
59
60

1
2
3 expected to remain the mainstay of modern toxicology testing strategies (National Research
4 Council 2007). The use of model cell lines from different origins and more than one cytotoxicity
5 assay is a reliable approach to systematically investigate the influence of NM properties on the
6 degrees and pathways of cytotoxicity (Bhattacharjee et al. 2013; Fröhlich et al. 2012;
7 Sohaebuddin et al. 2010). 3T3 cell model is considered very sensitive to verify *in vitro* cytotoxic
8 effects of NMs (Uboldi et al. 2012; Mahto et al. 2010), while HeLa tumor cell line is a culture
9 model widely used in cytotoxicity and especially in cell uptake studies of a broad range of
10 particulate nanocarriers (Kelsch et al. 2012; Salado et al. 2012). The tumor HeLa cell line was
11 more resistant to NV cytotoxic effects, which was in agreement with our previous study
12 (Nogueira et al. 2011b). These results are also in line with those reported by several authors
13 (Fröhlich et al. 2012; Müller et al. 1997; Schöler et al. 2001; Sohaebuddin et al. 2010; Xia et al.
14 2008), who noticed that the cytotoxic effects of particulate carrier systems differ depending on
15 the cell lines used, due to the innate nature, metabolic abilities (e.g. enzymes present) and
16 capabilities of the cell lines. In an attempt to understand the toxic response of NMs, here we
17 used different cytotoxicity assays. The higher sensitivity of the MTT assay for detecting the
18 cytotoxic effects of the NVs containing MKM and PKM suggests that the cytotoxicity primarily
19 originated at the mitochondrial compartment after cellular internalization of NVs rather than
20 physical damage to both lysosomal (NRU assay) and plasma (LDH assay) membranes (Yang et
21 al. 2009). Noteworthy is that the intracellular reactions of internalized NMs were reported to
22 lead to cellular metabolism/mitochondrial dysfunction (Horie et al. 2012). Concerning to cell
23 membrane integrity, we observed different effects when the cell line was varied, being NRU
24 assay more sensitive in HeLa cells and LDH in 3T3 fibroblasts. These results corroborated the
25 different interaction mechanisms of these NVs within cells from different origins and species. In
26 contrast, NVs formulated with MLM generally displayed the same level of cytotoxicity with the
27 three endpoints. These NVs have higher positive ZP in cell culture medium, which might
28
29
30
31
32
33
34
35
36
37
38
39
40
41
42
43
44
45
46
47
48
49
50
51
52
53
54
55
56
57
58
59
60

1
2
3 support their higher binding to the negatively charged lipid bilayer by electrostatic interaction
4
5 and, thus, their toxic effects on the cell membrane to the same extent as cell metabolism
6
7 depletion (Venkatesan et al. 2011; Xia et al. 2008). All in all, these results led to a key finding of
8
9 our research: the structural characteristic of the surfactant included in the NV directly affects its
10
11 cytotoxic effects. Firstly, the position of the cationic charge in the amphiphile molecule was
12
13 critical in determining the resulting formulation's cytotoxicity. Secondly, the hydrophobicity of
14
15 the surfactant was directly related to the NV toxic effects: the longer the alkyl chain of the
16
17 amphiphile, the higher the NV cytotoxicity. Based on the variability of cell responses, a
18
19 combination of cell lines and endpoints might be suitable for a reliable *in vitro* evaluation of
20
21 nanotoxicity. Finally, the small interference of the NVs with the MTT dye did not result in
22
23 further increase in cell viability with increasing NM concentration, which is in contrast to
24
25 previous reported data for other types of NMs (Monteiro-Riviere et al. 2009, 2010). These data
26
27 prove that these small interactions were no significant and, therefore, that the viability endpoints
28
29 are suitable for the intended purpose.
30
31
32
33

34 After showing that NVs exerted cytotoxic effects on the proliferation of fibroblasts in a
35
36 typically dose-dependent manner, we examined whether the induction of apoptosis was the
37
38 possible molecular mechanism involved in the cytotoxicity of NVs. Morphological alterations
39
40 detected after staining with AO/EB demonstrated that the NV treatments could induce apoptosis
41
42 in cultured fibroblasts. Whereas the apoptotic effects could be attributed to the observed
43
44 induction of oxidative damage (AshaRani et al. 2009), mitochondrial dysfunction, which can be
45
46 determined by MTT assay (Fisher et al. 2003), is reported as an intrinsic pathway of apoptosis.
47
48 Therefore, the apoptotic effects of the NVs containing especially MKM and PKM can be
49
50 directly related to oxidative stress and early mitochondrial injury. Additionally, plasma
51
52 membrane integrity modifications that are detected by LDH assay could be related to the late
53
54 stage of apoptosis (Fisher et al. 2003) and necrosis. Recent reports have identified apoptosis as a
55
56
57
58
59
60

1
2
3 major mechanism of cell death in exposure to NMs (Hsin et al. 2008; Pan et al. 2007). However,
4
5 in our case, although the number of apoptotic cells increased, most cells remained viable after
6
7 NV treatments. This suggests that other factors also contribute to cell death, aside from the
8
9 apoptotic pathway.
10

11
12 Toxicity studies were further extended to cell-cycle analysis, which showed that NV
13
14 treatment did not induce many significant alterations, as the cell cycle distribution was very
15
16 similar to the control. This suggests that cell cycle arrest is not the mechanism underlying NV
17
18 cytotoxicity. In this line, genotoxicity did not appear to be one of the main mechanisms involved
19
20 in NV toxic effects. Although some significant values of % Tail DNA were obtained with
21
22 respect to the negative control, the overall responses can be considered biologically non-
23
24 significant, as the % values were close to the negative control values and much lower than those
25
26 displayed by the positive MMS control. These results are in agreement with the cell cycle
27
28 analysis, as, if present, DNA damage would be evidenced in cell cycle progression with the
29
30 accumulation of cells in a determined cycle phase (AshaRani et al. 2009).
31
32

33
34 NMs might be able to disturb the oxidative balance in a cellular environment. This
35
36 phenomenon is called oxidative stress and results in abnormally large concentrations of
37
38 intracellular reactive oxygen species (ROS) (Marquis et al. 2009). In response to oxidative
39
40 stress, cell surface and organelle membrane lipids may undergo peroxidation (Choi et al. 2007).
41
42 A marker of lipid peroxidation elicited by ROS is increased MDA production, which was
43
44 induced by the NVs containing MKM or PKM. The inverse correlation between cell viability
45
46 and MDA level made the latter a key analytical marker for induced cell damage, which in turn
47
48 indicated that oxidative stress was probably a key route by which these NVs induce cytotoxicity.
49
50 ROS-induced membrane lipid peroxidation may occur both at cellular and organelle levels,
51
52 especially in the membranes of metabolically active mitochondria. This makes mitochondrial
53
54 injury a marker of elevated intracellular ROS level (Choi et al. 2007; Jones and Grainger 2009).
55
56
57
58
59
60

1
2
3 The early compromised cell viability detected by the MTT reduction assay may also result from
4 this insult.
5

6
7 Intravenous administration of a nanocarrier is limited by its hemolytic activity, among
8 other factors. Thus, hemolysis should be assessed to determine the biocompatibility of a material
9 (He et al. 2009). The low hemolytic activity of NVs at concentrations that were also non-
10 cytotoxic ($< 100 \mu\text{M}$) indicated the hemocompatibility of the formulations. Generally, a
11 percentage of hemolysis of less than 5% was regarded as non-toxic (He et al. 2009). Moreover,
12 the strong positive charge of the NVs did not induce erythrocyte agglutination. This is in
13 contrast to previous reported data for cationic carriers (Eliyahu et al. 2002), but corroborates the
14 hemocompatible properties of the NVs. The NVs were more toxic to 3T3 and HeLa cells than to
15 erythrocytes. This greater sensitivity may reflect differences in intrinsic structural properties of
16 membranes and might be attributed to the fact that erythrocytes cannot internalize foreign
17 particles, which leads to poor insertion into the phospholipid membrane and consequently low
18 hemolytic activity (Yessine et al. 2003). Furthermore, protein adsorption on particulate drug
19 carriers is regarded as a key factor for their *in vivo* fate and might also play an important role in
20 directing their cell uptake and toxicity (Dutta et al. 2007). Minimal differences in protein pattern
21 were observed after plasma incubation with NVs. This indicates that negligible or very small
22 amount of plasma protein was adsorbed onto NVs following incubation under *in vitro*
23 conditions. Overall, our results showed that the NVs positive charge, attributed to the surface
24 modification with cationic lysine-based amphiphiles, did not compromise the desirable blood
25 compatibility of the lipid-based vesicles.
26
27
28
29
30
31
32
33
34
35
36
37
38
39
40
41
42
43
44
45
46
47
48

49 The therapeutic effects of the drug-loaded NMs would firstly depend on internalization
50 by the diseased cells (Mei et al. 2009). Here, the observed punctuate distribution of fluorescence
51 in the cell cytosol indicated the cell uptake of the NR-NVs. The more intense fluorescence at 24
52 h indicated a higher cell uptake after a longer incubation time, whereas the diffuse fluorescence
53
54
55
56
57
58
59
60

1
2
3 in the cytosol can be attributed to dye release after endosome rupture. Internalization is probably
4
5 mediated through an endocytic pathway through non-specific interactions (e.g., adsorptive
6
7 endocytosis) with cell membrane (Park et al. 2006). Moreover, the results obtained after the
8
9 concomitant cell incubation with calcein and NV suggest that the NMs entered the cell by
10
11 endocytosis (see discussion below). Noteworthy is that the formation of secondary vesicles due
12
13 to aggregation in cell culture medium did not inhibited their cellular uptake. Finally, and in
14
15 relation to the toxic effects of NVs, the hydrophobicity (Arora et al. 2012) and the electrostatic
16
17 interactions between the cationic NVs and the anionic cell surface (Venkatesan et al. 2011)
18
19 might be responsible for the cell uptake.
20
21

22
23 The high efficiency of amphiphiles with a positive charge on the α -amino group of lysine
24
25 (MKM and PKM) at disrupting cell membranes within the pH range characteristic of late
26
27 endosomes (Nogueira et al. 2012a) prompted an evaluation of the ability of NVs containing
28
29 these compounds to release endocytosed materials into the cytoplasm of cells. One common
30
31 strategy for the intracellular delivery of encapsulated and/or intercalated material via lipid-based
32
33 vesicles exploits intracellular pH gradients (Pollock et al. 2010; Torchilin et al. 1993). We used
34
35 calcein as a tracer molecule, which is internalized by the cell through endocytosis and is used to
36
37 monitor the stability of endosomes following NM uptake (Hu et al. 2007). In the absence of
38
39 NVs, endosomal compartmentalization of calcein was observed, indicating that the endosome
40
41 membranes were not damaged (Chen et al. 2009; Hu et al. 2007). When the MLM was included
42
43 into the NVs, it was observed a different behavior depending on the composition of the basic
44
45 lipid membrane. Only the formulations without cholesterol had the ability to release some
46
47 calcein from endosomes, which can be due to a non specific interaction between these NVs and
48
49 the endosomal membrane. In contrast, the NVs containing MKM and PKM induced efficient
50
51 and greater release of endocytosed material into the cytoplasm regardless of the composition of
52
53 the lipid-based matrix. These results corroborated the pH-responsive membrane-lytic activity of
54
55
56
57
58
59
60

1
2
3 the latter surfactants demonstrated in our previous study (Nogueira et al. 2012a). Since MKM
4 and PKM are more protonated at acidic pH ($pK_a = 5.3$ and 4.5 , respectively), they might interact
5 with negatively-charged endosomal membranes, induce influx of water and ions, and eventually
6 bring about endosome destabilization and drug release (Park et al. 2006). The stronger diffuse
7 staining observed after cell treatment with the NVs containing MKM may be directly related to
8 the higher membrane-lytic activity of MKM at the pH range characteristic of the endosomal
9 compartments (Nogueira et al. 2012a). The efficient intracellular delivery of therapeutic
10 compounds into the cytosol by destabilizing endosomal membranes under mildly acidic
11 conditions would manipulate or circumvent non-productive trafficking from endosomes to
12 lysosomes, in which degradation may occur (Chen et al. 2009).

13
14 All considered, these data on the cytotoxic pathways and intracellular behavior show a
15 structure-activity relationship of the cellular events in response to NVs, which is summarized in
16 Table 3. The main finding is that the position of the cationic charge in surfactant molecule
17 determines the NV cytotoxic responses, induction of oxidative stress, endosomal release and
18 hemolytic activity. NVs containing the surfactants with cationic charge on the α -amino group of
19 lysine affect firstly the mitochondria, followed by the lysosomal and plasma membrane, as
20 demonstrated by the corresponding *in vitro* endpoints. Moreover, the surfactant hydrophobicity
21 correlates directly with the cytotoxic and genotoxic effects. In contrast, the surfactant chemical
22 structure does not affect the NV effects on apoptosis, cell cycle, erythrocyte agglutination and
23 plasma protein adsorption.

24
25 Finally, it is appropriate to comment on the importance of these findings for
26 nanotoxicology. Here, we showed that some NVs have the ability to lysis the endosomal
27 membrane and are therefore potential carriers for specific intracellular drug delivery. However,
28 we also demonstrated that they have an effect on normal cell biological functions and that such
29 effect is presented in terms of various toxic mechanisms. We must highlight the *in vitro*

1
2
3 approach used in this study as a reliable predictive model to provide an affordable database on
4
5 the biological activities of new NMs as a function of their chemical composition, which would
6
7 help understand their risks and opportunities before any *in vivo* application. An initial animal-
8
9 based screening approach is not feasible with regard to laboratory capacities and costs, and it
10
11 certainly is not desirable from an animal welfare viewpoint (Hartung 2010). Relevant *in vitro*
12
13 data may suggest the feasibility of new NMs for further applications. Therefore, only the NMs
14
15 with such relevance must be addressed for additional *in vivo* studies to corroborate the initial
16
17 hypothesis demonstrated through *in vitro* screening assays.
18
19

20 21 22 **Conclusions**

23
24 Here, we used an *in vitro* toxicological approach to elucidate the biological activity and
25
26 intracellular behavior of new cationic NV formulations containing biocompatible lysine-based
27
28 amphiphiles. We demonstrated the cell-specific nature of NV toxicity as well as different toxic
29
30 responses when the *in vitro* endpoint varied. A possible mechanism of toxicity is proposed
31
32 involving NV cell uptake followed by induction of oxidative stress, which in turn cause
33
34 mitochondrial dysfunction and ultimately result in apoptosis of cells. This mechanism is
35
36 especially proposed as the cytotoxicity pathway induced by the NVs containing MKM and
37
38 PKM, as those with MLM did not prompt significant oxidative stress and mitochondrial injury.
39
40 The cytotoxicity of the latter NVs seems to be attributed to an initial damage to the cell
41
42 membranes. NV cytotoxicity as well as their cellular uptake might be attributable to the cationic
43
44 charge. Our findings suggest that the cationic charge position and hydrophobicity of the
45
46 amphiphiles determine the NV interaction within the cell and, thus, their resulting toxicity and
47
48 intracellular behavior after cell uptake. NVs containing MKM and PKM (with a cationic charge
49
50 on the α -amino group of lysine) are especially recommended as pH-sensitive nanocarriers for
51
52 intracellular drug delivery. They have the ability to specifically lyse the endosome membrane in
53
54 mildly acidic conditions, as evidenced here and demonstrated in our preliminary study
55
56
57
58
59
60

1
2
3 (Nogueira et al. 2012a). Desirable blood compatibility was substantiated by minimal interaction
4
5 with erythrocytes and lack of plasma protein adsorption, which also corroborates the potential
6
7 application of these NVs as carriers of intravenous biomedical drugs that have their site of
8
9 action in the intracellular compartments. However, we are aware that further *in vivo* studies must
10
11 be conducted in this field to prove this hypothesis. Finally, as each NM type shows unique
12
13 physicochemical properties, the combination of assays used here, together with all the
14
15 information provided, offers an in-depth and comprehensive evaluation of the toxic effects of
16
17 novel NMs and contributes to reducing the uncertainty surrounding their potential health
18
19 hazards.
20
21

22 23 24 **Acknowledgments**

25
26 This research was supported by Projects CTQ2009-14151-C02-02 and CTQ2009-14151-C02-01
27
28 of the *Ministerio de Ciencia e Innovación* (Spain), and MAT2012-38047-C02-01 of the
29
30 *Ministerio de Economía y Competitividad* (Spain). We also thank Dr. Núria Cortadellas and Dr.
31
32 Jaume Comas for their expert technical assistance with the TEM and flow cytometry
33
34 experiments, respectively. Daniele Rubert Nogueira holds a PhD grant from MAEC-AECID
35
36 (Spain).
37
38
39
40

41 **Declaration of interest**

42
43 The authors state that they have no conflict of interest.
44
45
46
47
48
49
50
51
52
53
54
55
56
57
58
59
60

References

- Ahmad J, Ahamed M, Akhtar MJ, Alrokayan SA, Siddiqui M, Musarrat J, Al-Khedhairi AA. 2012. Apoptosis induction by silica nanoparticles mediated through reactive oxygen species in human liver cell line HepG2. *Toxicol Appl Pharmacol* 259:160-168.
- Arora S, Rajwade JM, Paknikar KM. 2012. Nanotoxicology and in vitro studies: The need of the hour. *Toxicol Appl Pharmacol* 258:151-165.
- AshaRani PV, Mun GLK, Hande MP, Valiyaveetil S. 2009. Cytotoxicity and genotoxicity of silver nanoparticles in human cells. *ACS Nano* 3:279-290.
- Bai W, Zhang Z, Tian W, He X, Ma Y, Zhao Y, Chai Z. 2009. Toxicity of zinc oxide nanoparticles to zebrafish embryo: a physicochemical study of toxicity mechanism. *J Nanopart Res* 12:1645-1654.
- Bhattacharjee S, Ershov D, van der Gucht J, Alink GM, Rietjens IMCM, Zuilhof H, Marcelis ATM. 2013. Surface charge-specific cytotoxicity and cellular uptake of tri-block copolymer nanoparticles. *Nanotoxicology* 7:71-84.
- Bombelli C, Caracciolo G, Di Profio P, Diociaiuti M, Luciani P, Mancini G, Mazzuca C, Marra M, Molinari A, Monti D, Toccaceli L, Venanzi M. 2005. Inclusion of a photosensitizer in liposomes formed by DMPC/Gemini Surfactant: Correlation between physicochemical and biological features of the complexes. *J Med Chem* 48:4882-4891.
- Bradford MM. 1976. A rapid and sensitive method for quantitation of microgram quantities of protein utilizing the principle of protein-dye binding. *Anal Biochem* 72:248-254.
- Cevc G. 2012. Rational design of new product candidates: The next generation of highly deformable bilayer vesicles for noninvasive, targeted therapy. *J Control Release* 160:135-146.
- Chen R, Khormae S, Eccleston ME, Slater NKH. 2009. The role of hydrophobic amino acid grafts in the enhancement of membrane-disruptive activity of pH-responsive pseudo-peptides. *Biomaterials* 30:1954-1961.
- Chen T, McIntosh D, He Y, Kim J, Tirrell DA, Scherrer P, Fenske D, Sandhu AP, Cullis PR. 2004. Alkylated derivatives of poly(ethylacrylic acid) can be inserted into preformed liposomes and trigger pH-dependent intracellular delivery of liposomal contents. *Mol Membr Biol* 21:385-393.

- 1
2
3 Choi AO, Cho SJ, Desbarats J, Lovric J, Maysinger D. 2007. Quantum dot-induced cell death
4 involves Fas upregulation and lipid peroxidation in human neuroblastoma cells. *J*
5 *Nanobiotechnol* 5:1.
6
7
8 Coldren B, van Zanten R, Mackel MJ, Zasadzinski J.A. 2003. From Vesicle Size Distributions
9 to Bilayer Elasticity via Cryo-Transmission and Freeze-Fracture Electron Microscopy.
10 *Langmuir* 19:5632-5639.
11
12
13 Collins TJ. 2007. ImageJ for microscopy. *BioTechniques* 43:S25-S30.
14
15
16 Colomer A, Pinazo A, Garcia T, Mitjans M, Vinardell P, Infante MR, Martínez V, Pérez L.
17 2012. pH sensitive surfactants from lysine: assessment of their cytotoxicity and environmental
18 behavior. *Langmuir* 28:5900-5912.
19
20
21 Dakwar GR, Hammad IA, Popov M, Linder C, Grinberg S, Heldman E, Stepensky D. 2012.
22 Delivery of proteins to the brain by bolaamphiphilic nao-sized vesicles. *J Control Release*
23 160:315-321.
24
25
26
27 Di Guglielmo C, De Lapuente J, Porredon C, Ramos-López D, Sendra J, Borràs M. 2012. In
28 *Vitro Safety Toxicology Data for Evaluation of Gold Nanoparticles—Chronic Cytotoxicity,*
29 *Genotoxicity and Uptake. J Nanosci Nanotechnol* 12:1-6.
30
31
32 Di Marzio L, Marianecchi C, Petrone M, Rinaldi F, Carafa M. 2011. Novel pH-sensitive non-
33 ionic surfactant vesicles: comparison between Tween 21 and Tween 20. *Colloids Surf B*
34 *Biointerfaces* 82 :18-24.
35
36
37
38 Dutta D, Sundaram SK, Teegarden JG, Riley BJ, Fifield LS, Jacobs JM. 2007. Adsorbed
39 proteins influence the biological activity and molecular targeting of nanomaterials. *Toxicol*
40 *Sci* 100:303-315.
41
42
43 Eliyahu H, Serval N, Domb AJ, Barenholz Y. 2002. Lipoplex-induced hemagglutination:
44 potential involvement in intravenous gene delivery. *Gene Ther* 9:850-858.
45
46
47 Fisher D, Li Y, Ahlemeyer B, Krieglstein J, Kissel T. 2003. In vitro cytotoxicity testing of
48 polycations: influence of polymer structure on cell viability and hemolysis. *Biomaterials*
49 24:1121-1131.
50
51
52
53 Fröhlich E, Meindl C, Roblegg E, Griesbacher A, Pieber TR. 2012. Cytotoxicity of
54 nanoparticles is influenced by size, proliferation and embryogenic origin of the cells used for
55 testing. *Nanotoxicology* 6:424-439.
56
57
58
59
60

- 1
2
3 Gao F, Cai Y, Zhou J, Xie X, Ouyang W, Zhang Y, Wang X, Zhang X, Wang X, Zhao L, Tang
4 J. 2010. Pullulan acetate coated magnetic nanoparticles for hyperthermia: preparation,
5 characterization and *in vitro* experiments. *Nano Res* 3:23-31.
6
7
8 Hartung T. 2010. Food and thought....on alternative methods for nanoparticle safety testing.
9 *ALTEX* 27:87-95.
10
11 He M, Zhao Z, Yin L, Tang C, Yin C. 2009. Hyaluronic acid coated poly(butyl cyano-acrylate)
12 nanoparticles as anticancer drug carriers. *Int J Pharm* 373:165-173.
13
14
15 Horie M, Kato H, Fujita K, Endoh S, Iwahashi H. 2012. *In vitro* evaluation of cellular response
16 induced by manufactured nanoparticles. *Chem Res Toxicol* 25:605-619.
17
18
19 Hsin YH, Chen CF, Huang S, Shih TS, Lai PS, Chueh PJ. 2008. The apoptotic effect of
20 nanosilver is mediated by a ROS- and JNK-dependent mechanism involving the
21 mitochondrial pathway in NIH3T3 cells. *Toxicol Lett* 179:130-139.
22
23
24
25 Hu Y, Litwin T, Nagaraja AR, Kwong B, Katz J, Watson N, Irvine DJ. 2007. Cytosolic delivery
26 of membrane-impermeable molecules in dendritic cells using pH-responsive core-shell
27 nanoparticles. *Nano Lett* 7:3056-3064.
28
29
30
31 Infante MR, Pérez L, Morán MC, Pons R, Mitjans M, Vinardell MP, Garcia MT, Pinazo A.
32 2010. Biocompatible surfactants from renewable hydrophiles. *Eur J Lipid Sci Technol*
33 112 :110-121.
34
35
36
37 Jones RA, Cheung CY, Black FE, Zia JK, Stayton PS, Hoffman AS, Wilson MR. 2003. Poly(2-
38 alkylacrylic acid) polymers deliver molecules to the cytosol by pH-sensitive disruption of
39 endosomal vesicles. *Biochem J* 372:65-75.
40
41
42 Jones CF, Grainger DW. 2009. *In vitro* assessments of nanomaterial toxicity. *Adv Drug Deliv*
43 *Rev* 61:438-456.
44
45
46 Kelsch A, Tomcin S, Rausch K, Barz M, Mailänder V, Schmidt M, Landfester K, Zentel R.
47 2012. HEMA copolymers as surfactants in the preparation of biocompatible nanoparticles for
48 biomedical application. *Biomacromolecules* 13:4179-4187.
49
50
51 Liang C-H, Chou T-H. 2009. Effect of chain length on physicochemical properties and
52 cytotoxicity of cationic vesicles composed of phosphatidylcholines and
53 dialkyldimethylammonium bromides. *Chem Phys Lip* 158:81-90.
54
55
56
57
58
59
60

- 1
2
3 Lundberg D, Faneca H, Morán MC, Lima MCP, Miguel MG, Lindman B. 2011. Inclusion of a
4 single-tail amino acid-based amphiphile in a lipoplex formulation: Effects on transfection
5 efficiency and physicochemical properties. *Mol Membr Biol* 28:42-53.
6
7
8 Mahto SK, Park C, Yoon TH, Rhee SW. 2010. Assessment of cytocompatibility of surface-
9 modified CdSe/ZnSe quantum dots for BALB/3T3 fibroblast cells. *Toxicol in vitro* 24:1070-
10 1077.
11
12
13 Marquis BJ, Love SA, Braun KL, Haynes CL. 2009. Analytical methods to assess nanoparticle
14 toxicity. *Analyst* 134:425-439.
15
16
17 Mehrotra A, Nagarwal RC, Pandit JK. 2011. Lomustine loaded chitosan nanoparticles:
18 characterization and in-vitro cytotoxicity on human luna cancer cell line L132. *Chem Pharm*
19 *Bull* 59:315-320.
20
21
22 Mei L, Zhang Y, Zheng Y, Tian G, Song C, Yang D, Chen H, Sun H, Tian Y, Liu K, Li Z,
23 Huang L. 2009. A novel docetaxel-loaded poly (ϵ -caprolactone)/pluronic F68 nanoparticle
24 overcoming multidrug resistance for breast cancer treatment. *Nanoscale Res Lett* 4:1530-
25 1539.
26
27
28 Monteiro-Riviere NA, Inman AO, Zhang LW. 2009. Limitations and relative utility of screening
29 assays to assess engineered nanoparticle toxicity in a human cell line. *Toxicol Appl*
30 *Pharmacol* 234:222-235.
31
32
33 Monteiro-Riviere NA, Oldenburg SJ, Inman AO. 2010. Interactions of aluminum nanoparticles
34 with human epidermal keratinocytes. *J Appl Toxicol* 30:276-285.
35
36
37 Morán MC, Infante MR, Miguel MG, Lindman B, Pons R. 2010. Novel Biocompatible DNA
38 Gel Particles. *Langmuir* 26:10606-10613.
39
40
41 Müller RH, Jacobs C, Kayser O. 2011. Nanosuspensions as particulate drug formulations in
42 therapy. Rationale for development and what we can expect for the future. *Adv Drug Deliv*
43 *Rev* 23:3-19.
44
45
46 Müller RH, Rühl D, Runge SA, Schulze-Forster K, Mehnert W. 1997. Cytotoxicity of solid lipid
47 nanoparticles as a function of the lipid matrix and the surfactant. *Pharm Res* 14:458-462.
48
49
50 National Research Council (2007). Toxicity testing in the twenty-first century: a vision and
51 strategy. National Academy Press, Washington, DC.
52
53
54
55
56
57
58
59
60

- 1
2
3 Nogueira DR, Mitjans M, Infante MR, Vinardell MP. 2011a. The role of counterions in the
4 membrane-disruptive properties of pH-sensitive lysine-based surfactants. *Acta Biomater*
5 7:2846-2856.
6
7
8 Nogueira DR, Mitjans M, Infante MR, Vinardell MP. 2011b. Comparative sensitivity of tumor
9 and non-tumor cell lines as a reliable approach for *in vitro* cytotoxicity screening of lysine-
10 based surfactants with potential pharmaceutical applications. *Int J Pharm* 420:51-58.
11
12
13 Nogueira DR, Mitjans M, Morán MC, Pérez L, Vinardell MP. 2012a. Membrane-destabilizing
14 activity of pH-responsive cationic lysine-based surfactants: role of charge position and alkyl
15 chain length. *Amino Acids* 43:1203-1215.
16
17
18 Nogueira DR, Mitjans M, Busquets MA, Pérez L, Vinardell MP. 2012b. Phospholipid bilayer
19 perturbing-properties underlying lysis induced by pH-sensitive cationic lysine-based
20 surfactants in biomembranes. *Langmuir* 28:11687-11698.
21
22
23 Nogueira DR, Morán MC, Mitjans M, Martínez V, Pérez L, Vinardell MP. 2013. New cationic
24 nanovesicular systems containing lysine-based surfactants for topical administration: toxicity
25 assessment using representative skin cell lines. *Eur J Pharm Biopharm* 83:33-43.
26
27
28 Ojogun VA, Lehmler H-J, Knutson BL. 2009. Cationic-anionic vesicle templating from
29 fluorocarbon/fluorocarbon and hydrocarbon/fluorocarbon surfactants. *J Coll Interf Sci*
30 338:82-91.
31
32
33 Paillard A, Hindré F, Vignes-Colombeix C, Benoit J-P, Garcion E. 2010. The importance of
34 endo-lysosomal escape with lipid nanocapsules for drug subcellular bioavailability.
35 *Biomaterials* 31:7542-7554.
36
37
38 Pan Y, Neuss S, Leifert A, Fischler M, Wen F, Simon U, Schmid G, Brandau W, Jahnen-
39 Dechent W. 2007. Size-dependent cytotoxicity of gold nanoparticles. *Small* 3:1941-1949.
40
41
42 Park JS, Han TH, Lee KY, Han SS, Hwang JJ, Moon DH, Kim SY, Cho YW. 2006. *N*-acetyl
43 histidine-conjugated glycol chitosan self-assembled nanoparticles for intracytoplasmic
44 delivery of drugs: endocytosis, exocytosis and drug release. *J Control Release* 115:37-45.
45
46
47 Pérez L, Pinazo A, García MT, Lozano M, Manresa A, Angelet M, Vinardell MP, Mitjans M,
48 Pons R, Infante MR. 2009. Cationic surfactants from lysine: Synthesis, micellization and
49 biological evaluation. *Eur J Med Chem* 44:1884-1892.
50
51
52
53
54
55
56
57
58
59
60

- 1
2
3 Pollock S, Antrobus R, Newton L, Kampa B, Rossa J, Latham S, Nichita NB, Dwek RA,
4 Zitzmann N. 2010. Uptake and trafficking of liposomes to the endoplasmic reticulum. *FASEB*
5 *J* 24:1866-1878.
6
7
8 Ramezani M, Khoshhamdam M, Dehshahri A, Malaekheh-Nikouei B. 2009. The influence of
9 size, lipid composition and bilayer fluidity of cationic liposomes on the transfection efficiency
10 of nanolipoplexes. *Colloids Surf B Biointerfaces* 72:1-5.
11
12 Rasband W, (1997). ImageJ. National Institutes of Health, Bethesda, MD, USA. Available at:
13 <http://rsbweb.nih.gov/ij/index.html>. Accessed on 9 January 2013
14
15
16
17 Robbens J, Vanparys C, Nobels I, Blust R, Hoecke KV, Janssen C, Schamphelaere KD, Roland
18 K, Blanchard G, Silvestre F, Gillardin V, Kestemont P, Anthonissen R, Toussaint O,
19 Vankoningsloo S, Saout C, Alfaro-Moreno E, Hoet P, Gonzalez L, Dubruel P, Troisfontaines
20 P. 2010. Eco-, geno-, and human toxicology of bio-active nanoparticles for biomedical
21 applications. *Toxicology* 269:170-181.
22
23
24
25
26 Salado J, Insausti M, Lezama L, Gil de Muro I, Moros M, Pelaz B, Grazu V, Fuente JM, Rojo T.
27 2012. Functionalized Fe₃O₄@Au superparamagnetic nanoparticles: in vitro bioactivity.
28 *Nanotechnology* 23:315102.
29
30
31
32 Schöler N, Olbrich C, Tabatt K, Müller RH, Hahn H, Liesenfeld O. 2001. Surfactant, but not the
33 size of solid lipid nanoparticles (SLN) influences viability and cytokine production of
34 macrophages, *Int J Pharm* 221:57-67.
35
36
37 Simões S, Moreira JN, Fonseca C, Düzgünes N, Lima MC. 2004. On the formulation of pH-
38 sensitive liposomes with long circulation times. *Adv Drug Deliv Rev* 56:947-965.
39
40
41 Singh NP, McCoy MT, Tice EL, Schneider EL. 1988. A simple technique for quantitation of
42 low levels of DNA damage in individual cells. *Exp Cell Res* 175:184-191.
43
44
45 Sohaebuddin SK, Thevenot PT, Baker D, Eaton JW, Tang L. 2010. Nanomaterial cytotoxicity is
46 composition, size, and cell type dependent. *Part Fibre Toxicol* 7:22.
47
48
49 Squier MKT, Cohen JJ. 2001. Standard quantitative assays for apoptosis. *Mol Biotechnol*
50 19:305-312.
51
52
53 Torchilin VP, Zhou F, Huang L. 1993. pH-sensitive liposomes. *J Liposome Res* 3:201-255.
54
55 Uboldi C, Giudetti G, Broggi F, Gilliland D, Ponti J, Rossi F. 2012. Amorphous silica
56 nanoparticles do not induce cytotoxicity, cell transformation or genotoxicity in Balb/3T3
57 mouse fibroblasts. *Mutat Res* 745:11-20.
58
59
60

- 1
2
3 Venkatesan P, Puvvada N, Dash R, Kumar BNP, Sarkar D, Azab B, Pathak A, Kundu SC,
4 Fisher PB, Mandal M. 2011. The potential of celecoxib-loaded hydroxyapatite-chitosan
5 nanocomposite for the treatment of colon cancer. *Biomaterials* 32:3794-3806.
6
7
8 Xia T, Kovoichich M, Liang M, Zink JI, Nel AE. 2008. Cationic polystyrene nanosphere toxicity
9 depends on cell-specific endocytic and mitochondrial injury pathways. *ACSNano* 2:85-96.
10
11 Yang H, Liu C, Yang D, Zhang H, Xi Z. 2009. Comparative study of cytotoxicity, oxidative
12 stress and genotoxicity induced by four typical nanomaterials: the role of particle size, shape
13 and composition. *J Appl Toxicol* 29:69-78.
14
15
16
17 Yessine MA, Lafleur M, Meier C, Petereit HU, Leroux JC. 2003. Characterization of the
18 membrane-destabilization properties of different pH-sensitive methacrylic acid copolymers.
19 *Biochim Biophys Acta* 1613:28-38.
20
21
22
23 Zhang SB, Xu YM, Wang B, Qiao WH, Liu DL, Li ZS. 2004. Cationic compounds used in
24 lipoplexes and polyplexes for gene delivery. *J Control Release* 100:165-180.
25
26
27
28
29
30
31
32
33
34
35
36
37
38
39
40
41
42
43
44
45
46
47
48
49
50
51
52
53
54
55
56
57
58
59
60

Figure captions:

Figure 1. Cell viability measured by the MTT (a-c) and NRU (d,e) assays, and cytotoxicity expressed by LDH release (f,g) on 3T3 (a,b,d,f) and HeLa (c,e,g) cell lines. The cells were exposed to increasing concentrations of the surfactants only (a) or of the NV formulations (b-g), ranging from 0.5 to 100 μ M. Results of MTT and NRU assays are given as a percentage of untreated control cells, whereas the cytotoxicity by LDH release was calculated in relation to the positive control set as 100% LDH release. The discontinuous straight line in each graph corresponds to untreated control cells set as 100% cell viability (MTT and NRU) or to positive control cells set as 100% cell death (LDH). Results are expressed as mean \pm SEM of three independent experiments, performed in triplicate. **The data on 3T3 cells for the NVs containing the surfactants are reprinted and adapted from Nogueira et al. 2013, with permission from Elsevier.**

Figure 2. Effect of various cationic NVs on apoptosis of 3T3 cells determined by fluorescence microscopy after AO and BE staining. (a) Per cent of viable, apoptotic and necrotic cells after 24 h treatment with the IC₅₀ concentrations (calculated by MTT assay) of each NV formulation. Fluorescent micrographs of (b) untreated control cells, (c) DMPC:MKM, (d) DMPC:CHOL:MKM and (e) DMPC:PKM. Legends: (►) typical live nuclei, (▼) chromatin condensation (early apoptosis), (▲) blebbing and nuclear margination (early to moderate apoptosis), (*) necrosis, (**) late apoptosis. Scale bar: 50 μ m.

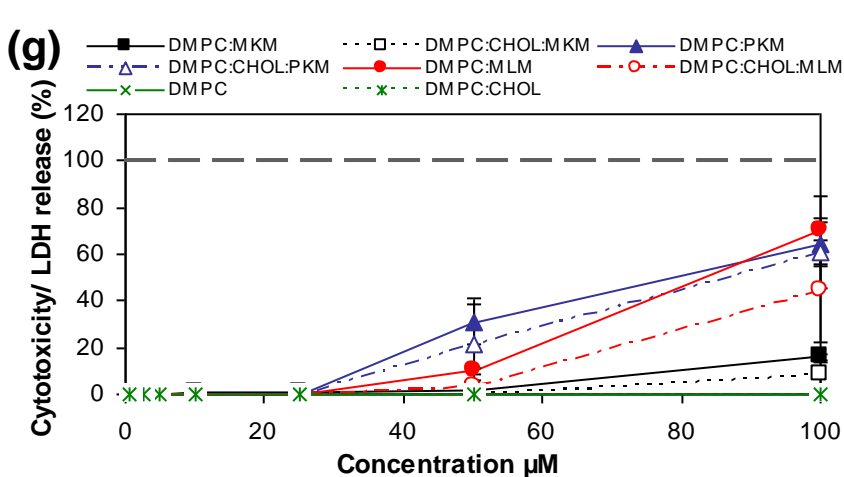
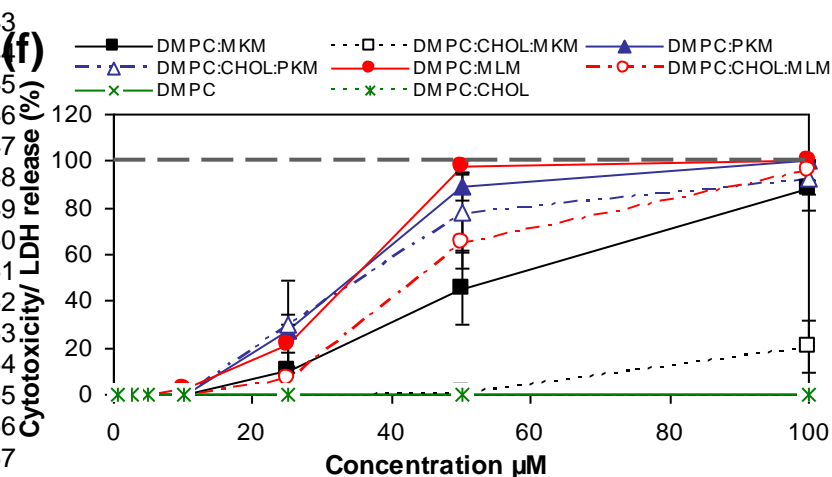
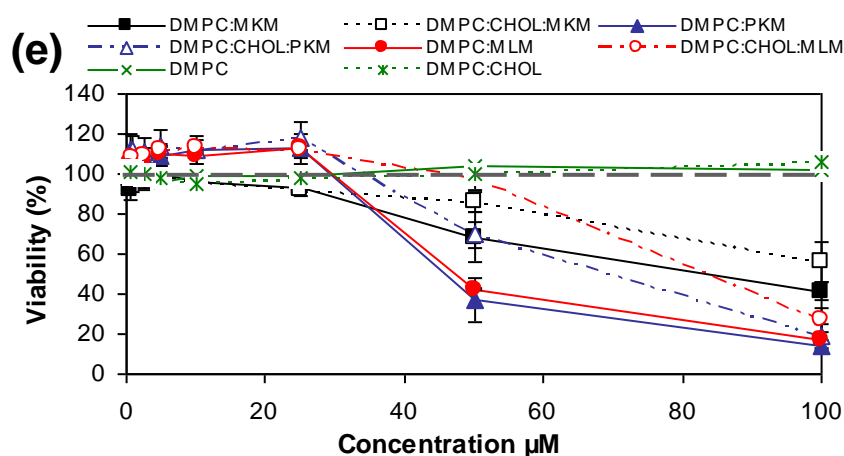
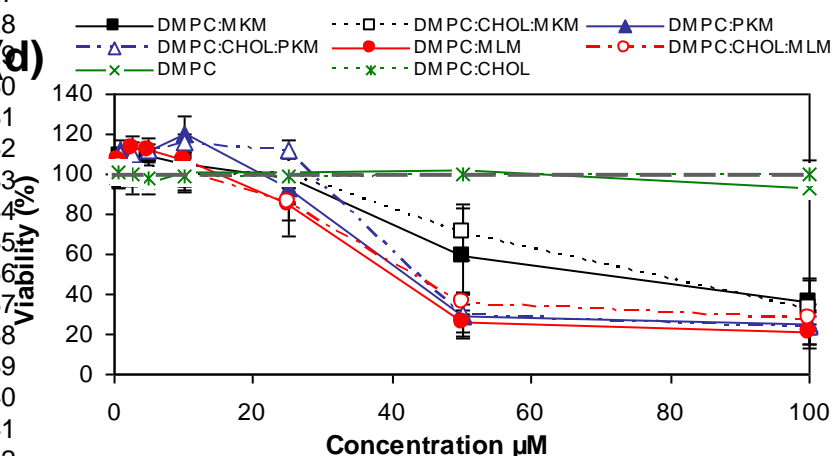
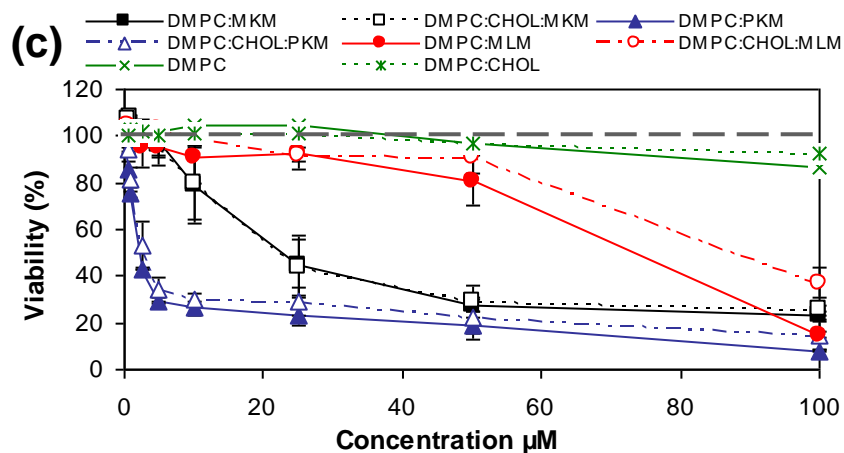
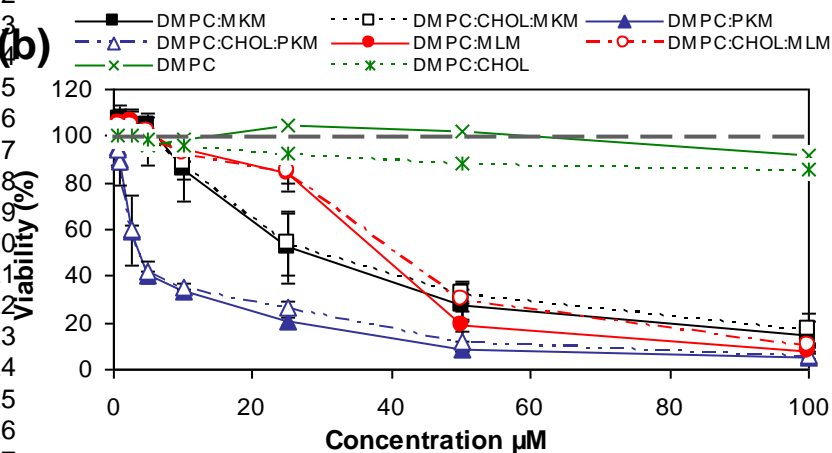
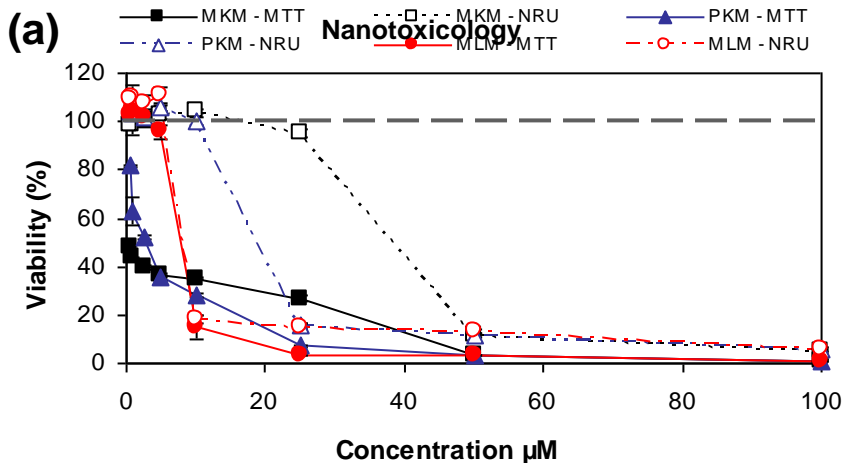
Figure 3. Cell-cycle analysis of 3T3 cells following 24 h treatment with IC₂₀ and IC₅₀ concentrations of each NV formulation. NVs containing (a) MKM, (b) PKM and (c) MLM. Results are expressed as mean \pm SEM of three independent experiments, performed in duplicate. Statistical analyses were performed using ANOVA followed by Dunnett's multiple comparison test. * $p < 0.05$, ** $p < 0.005$ denote significant differences.

Figure 4. DNA damage in 3T3 cells determined by a comet assay. The cells were treated for 24 h with the IC₁₀, IC₂₀ and IC₃₀ concentrations (calculated by MTT assay) of each NV formulation. Fluorescent micrographs of (a) untreated control cells, (b) cells treated with 400 μ M of MMS (positive control) and (c) cells treated with IC₂₀ of DMPC:CHOL:PKM. Scale bar: 50 μ m. (d) % Tail DNA. Values shown are the mean of 50 randomly selected comet images of each sample \pm SEM. Statistical analyses were performed using ANOVA followed by Dunnett's multiple comparison test. * $p < 0.005$ denotes significant differences.

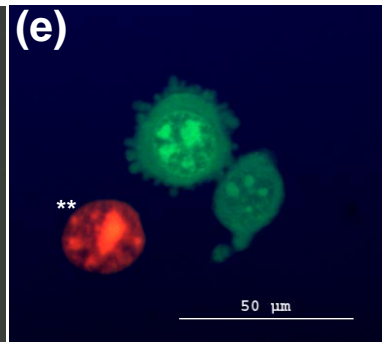
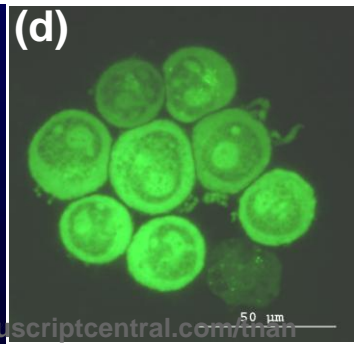
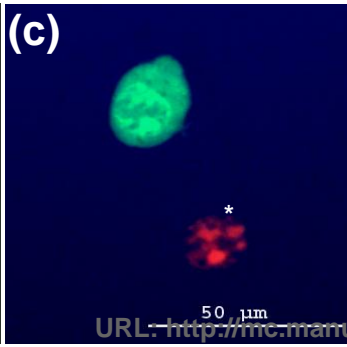
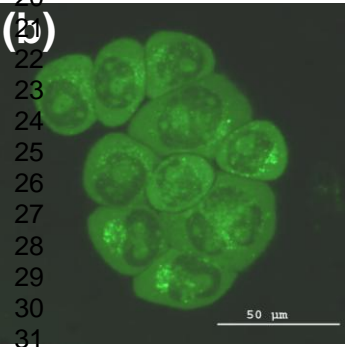
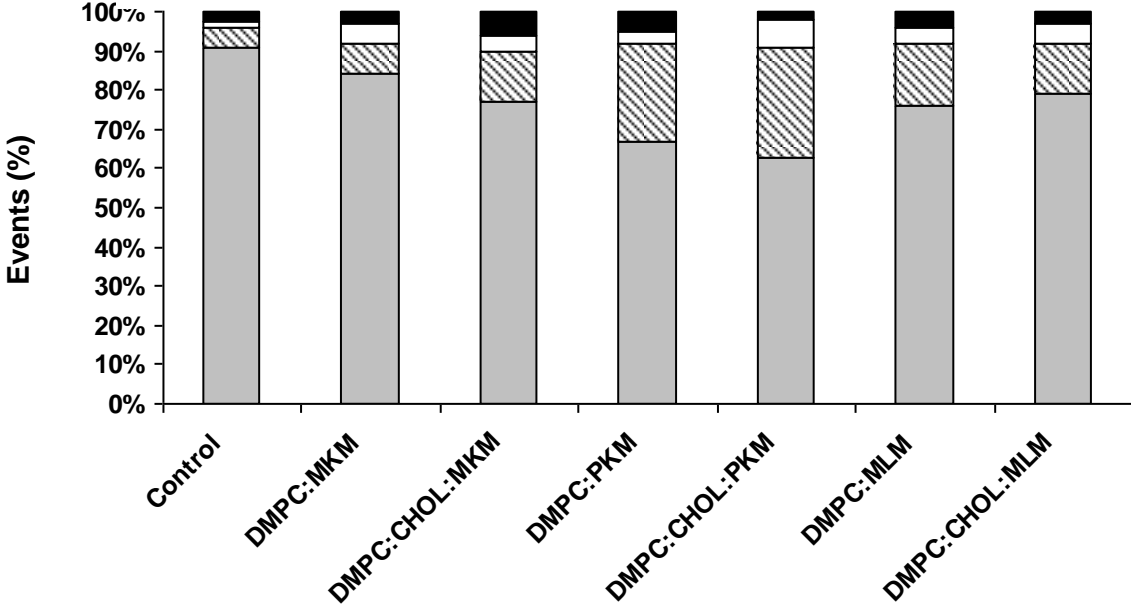
1
2
3 **Figure 5.** Quantitative analysis of MDA concentrations after exposure of 3T3 cells for 24 h to
4 the IC₅₀ concentrations of each NV formulation. MDA is a marker of lipid peroxidation and,
5 thus, of cellular oxidative stress. Results are expressed as mean ± SEM of three independent
6 experiments, performed in duplicate. Statistical analyses were performed using ANOVA
7 followed by Dunnett's multiple comparison test. * p < 0.05, ** p < 0.005 denote significant
8 differences.
9
10
11
12

13 **Figure 6.** Blood compatibility of NVs. (a) Percentage of hemolysis caused by NVs after 1 h of
14 incubation with rat erythrocytes. Each value represents the mean ± SEM of three experiments.
15 Agglutination of rat erythrocytes observed by phase microscopy after 1h of incubation with 100
16 μM of each NV formulation: (b) control, (c) DMPC:MKM, (d) DMPC:CHOL:MKM, (e)
17 DMPC:PKM, (f) DMPC:CHOL:PKM, (g) DMPC:MLM, (h) DMPC:CHOL:MLM. Scale bar:
18 100 μm. Plasma protein adsorption assessed by SDS-PAGE: (i) protein present in the
19 supernatant and (j) protein adsorbed to the NVs after incubation of 10% plasma with 100 μM of
20 each NV formulation for 1 h at 37°C. 1 = DMPC:PKM, 2 = DMPC:CHOL:PKM, 3 =
21 DMPC:MKM, 4 = DMPC:CHOL:MKM, 5 = DMPC:MLM, 6 = DMPC:CHOL:MLM, C =
22 control 10% plasma, i and ii = wash fluids from DMPC:PKM and DMPC:MKM samples,
23 respectively.
24
25
26
27
28
29
30
31

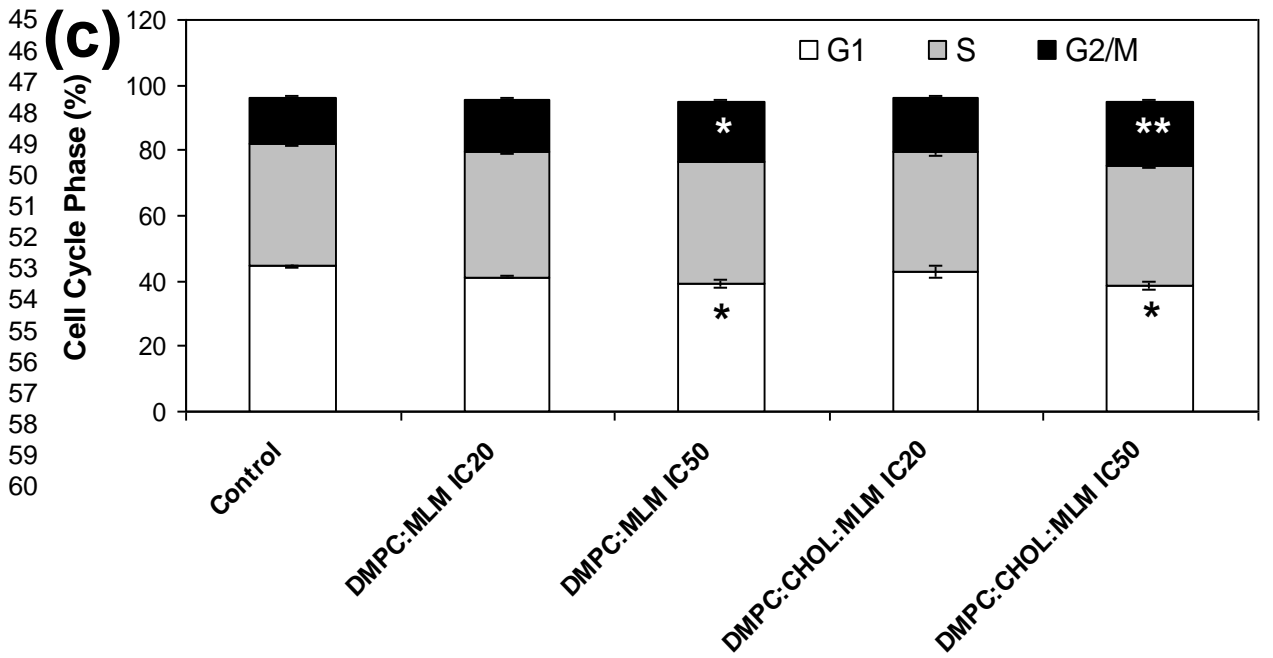
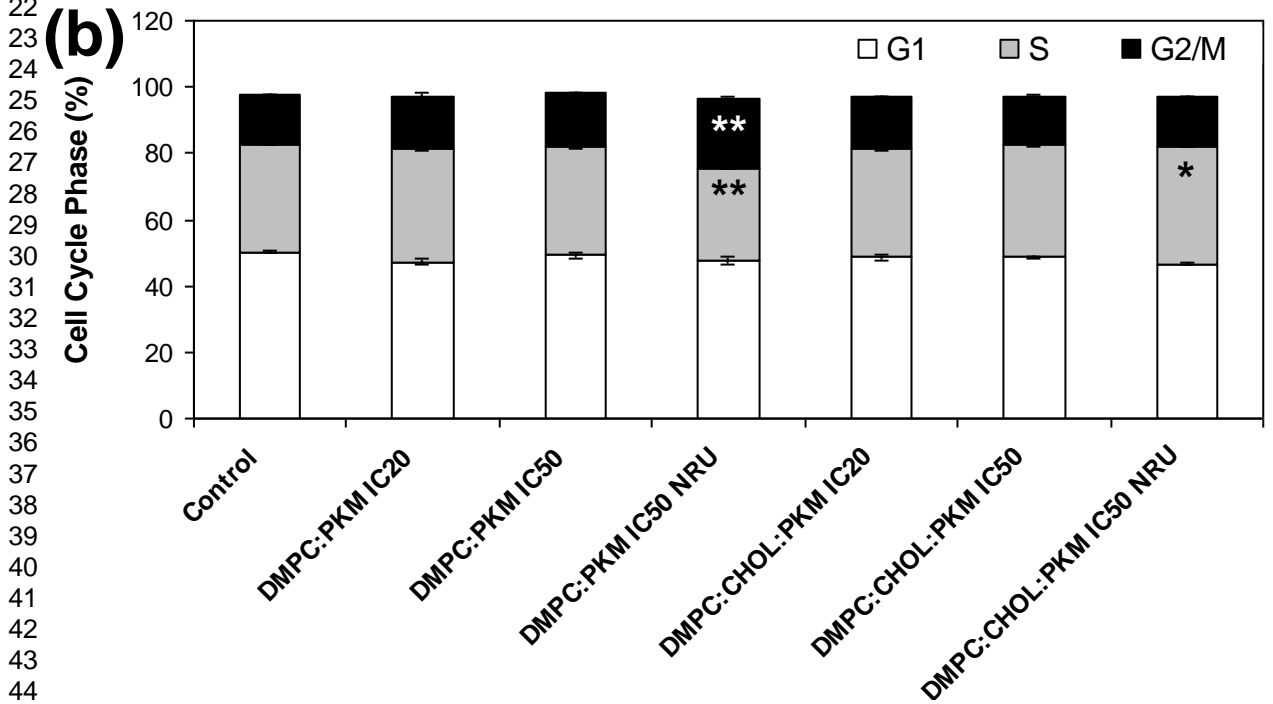
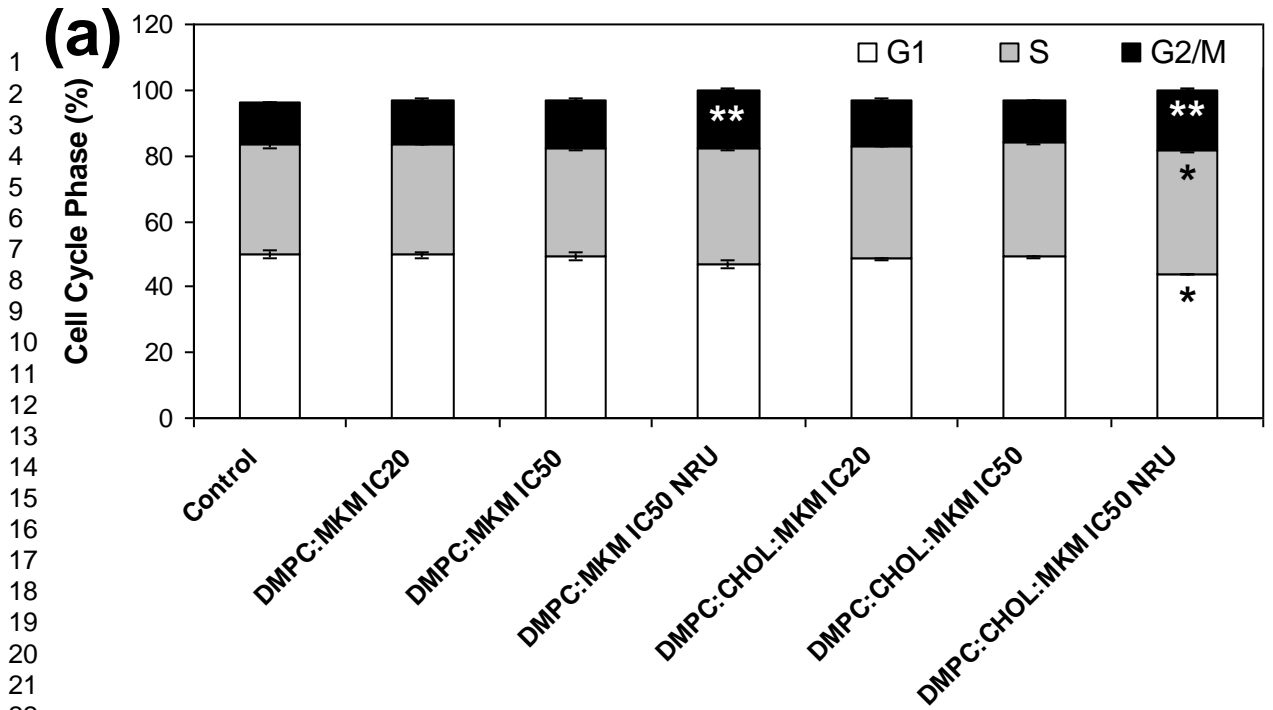
32 **Figure 7.** (A) Localization of NR-NVs (DMPC:MKM) by HeLa cells after 2h and 24 h of
33 incubation at 37°C. Cell uptake is visualized using fluorescence microscopy. (B) Fluorescence
34 microscopy images of HeLa cells showing the subcellular distribution of calcein fluorescence.
35 The cells were treated with 1 mg/ml calcein (control), and both 1 mg/ml calcein and 50 μM of
36 each NV formulation. Images were acquired at 3 h after 1 h of uptake. Scale bar: 50 μm. (C)
37 Quantitative fluorescence analysis of images like those in 'A' and (D) of images like those in
38 'B'. The results represent the mean of values determined for ~20 cells ± SEM. See the Materials
39 and Methods section for details of the analysis performed. Statistical analyses were performed
40 using Student's *t* test (⁺⁺ p < 0.005) or ANOVA followed by Dunnett's multiple comparison test
41 (* p < 0.05 and ** p < 0.005).
42
43
44
45
46
47
48
49
50
51
52
53
54
55
56
57
58
59
60

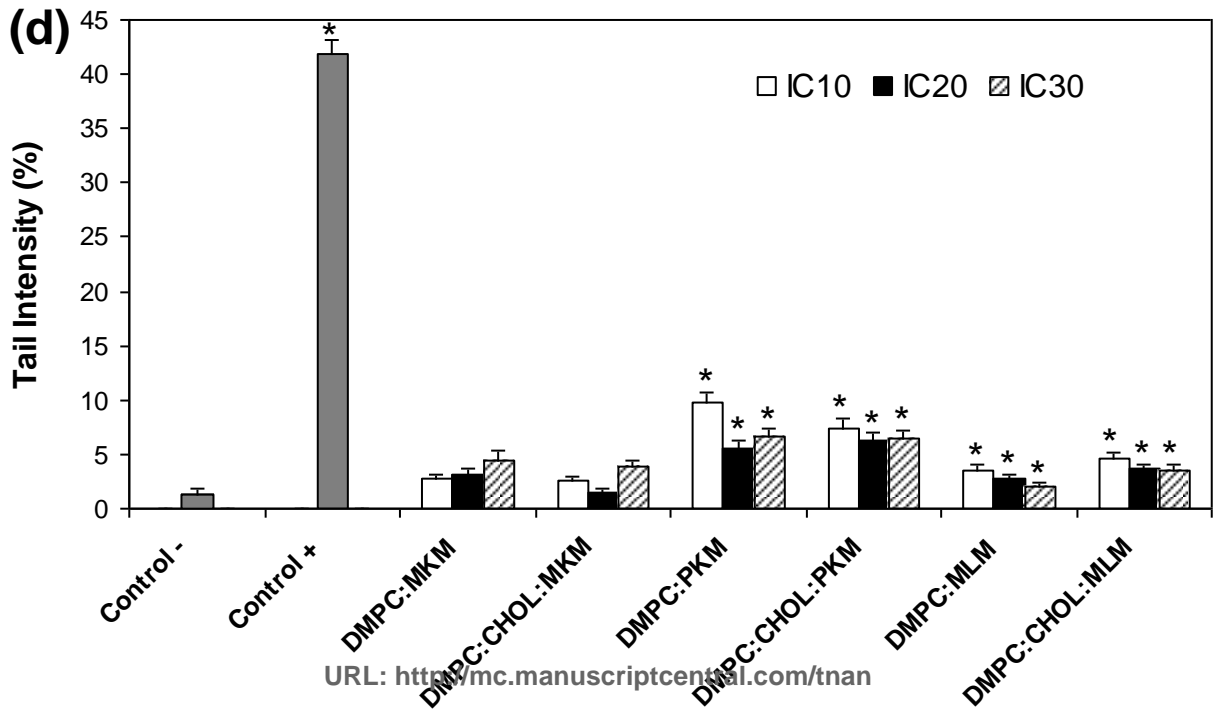
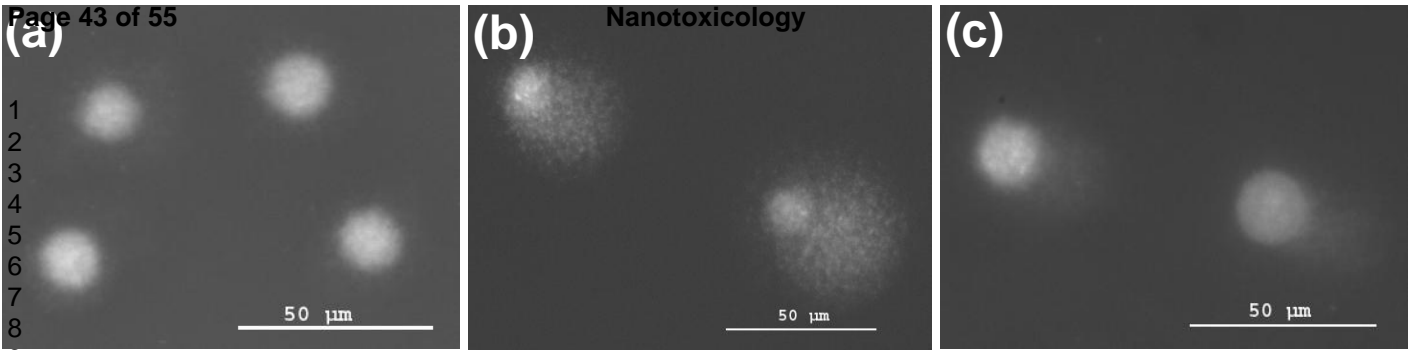


Nanotoxicology
■ Normal cells ▨ Apoptosis □ Late Apoptosis ■ Necrosis

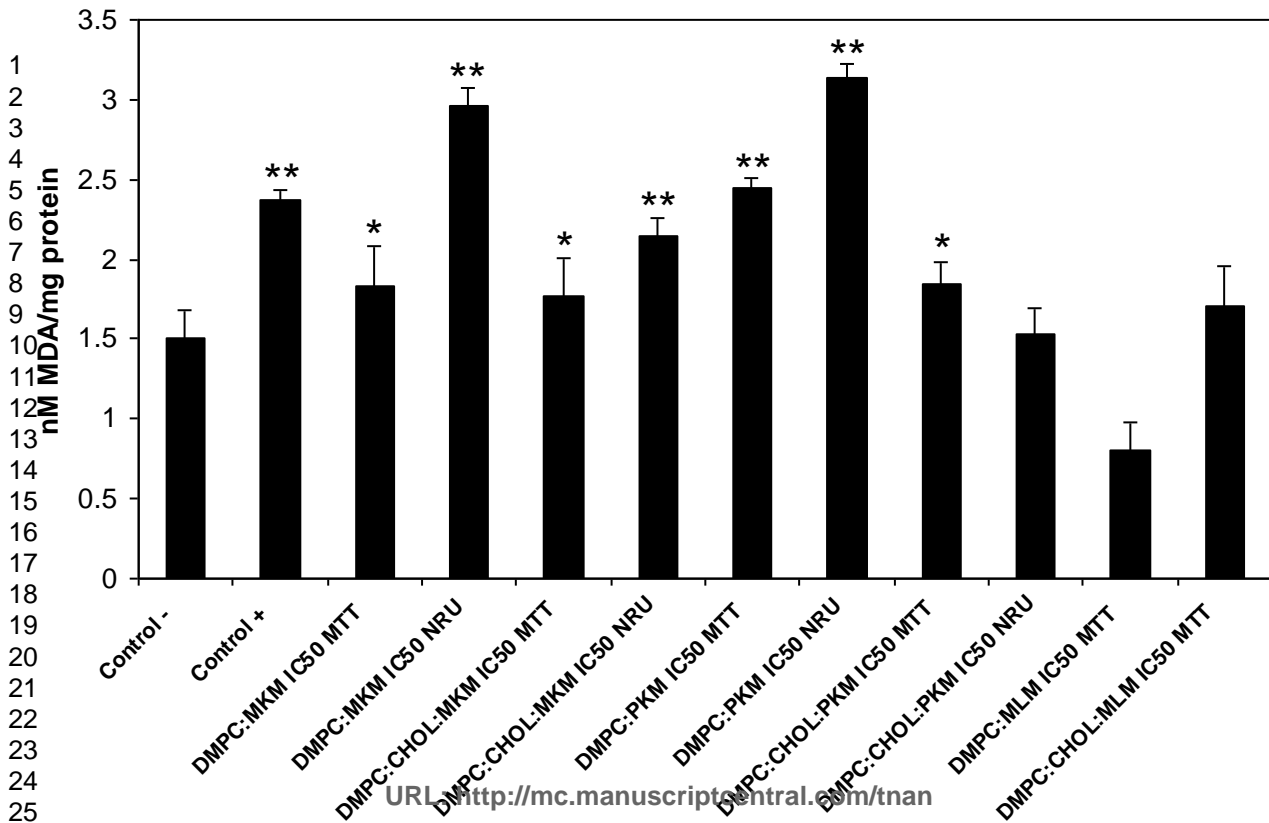


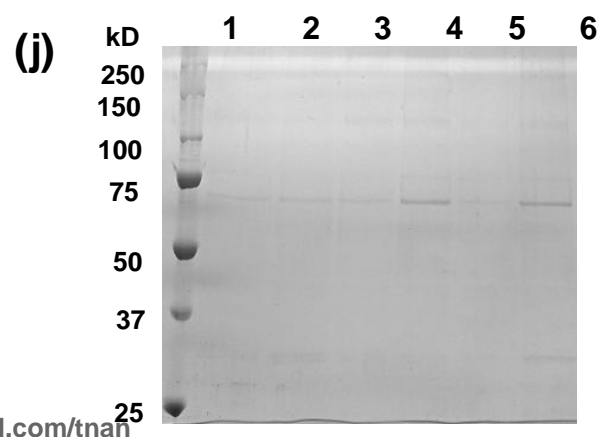
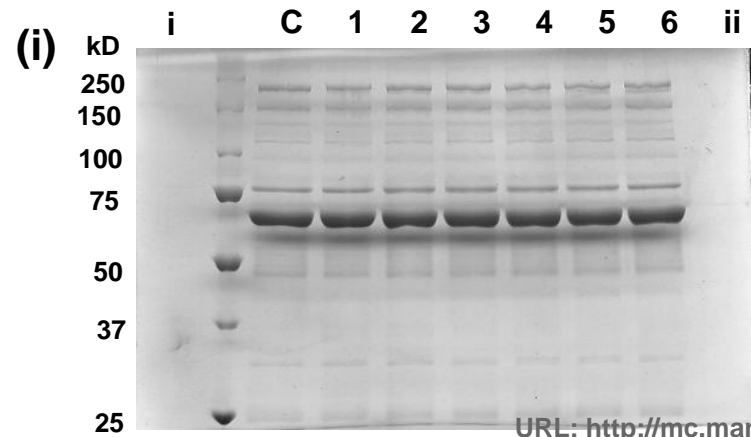
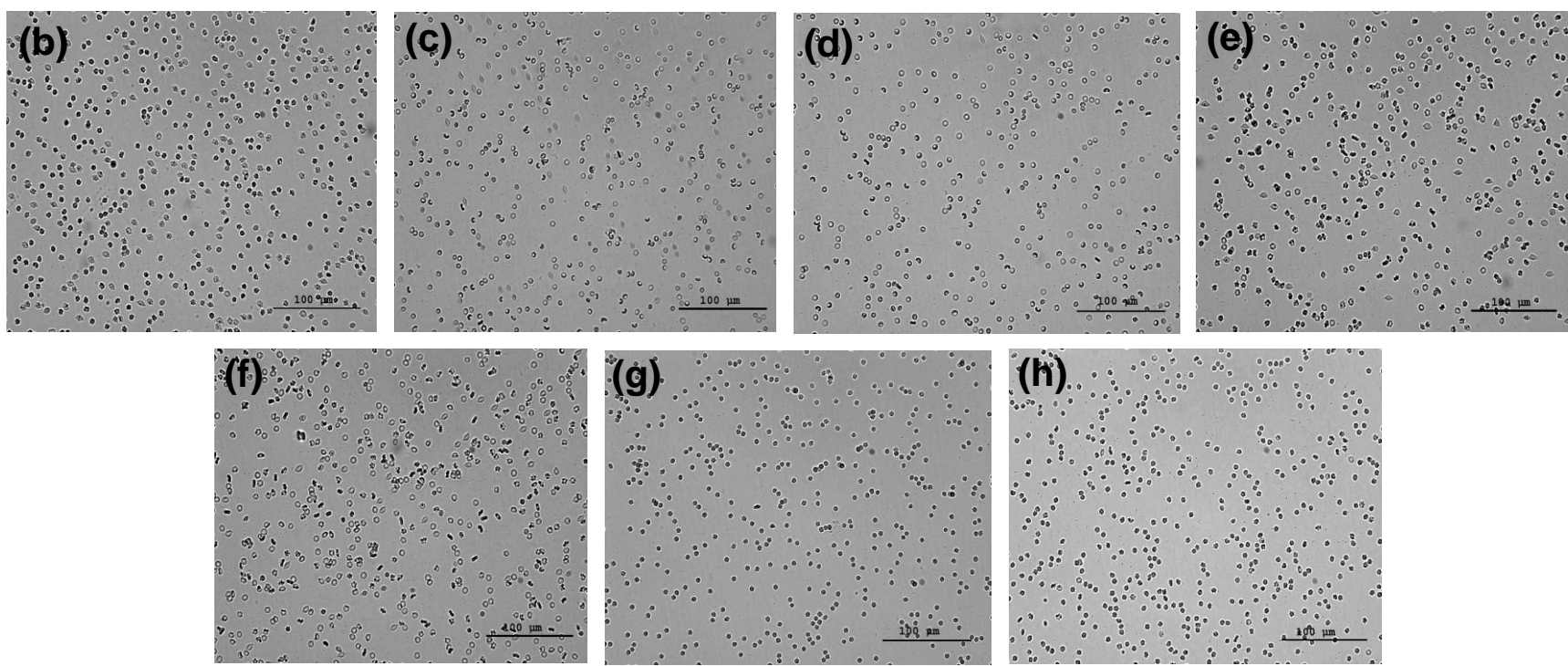
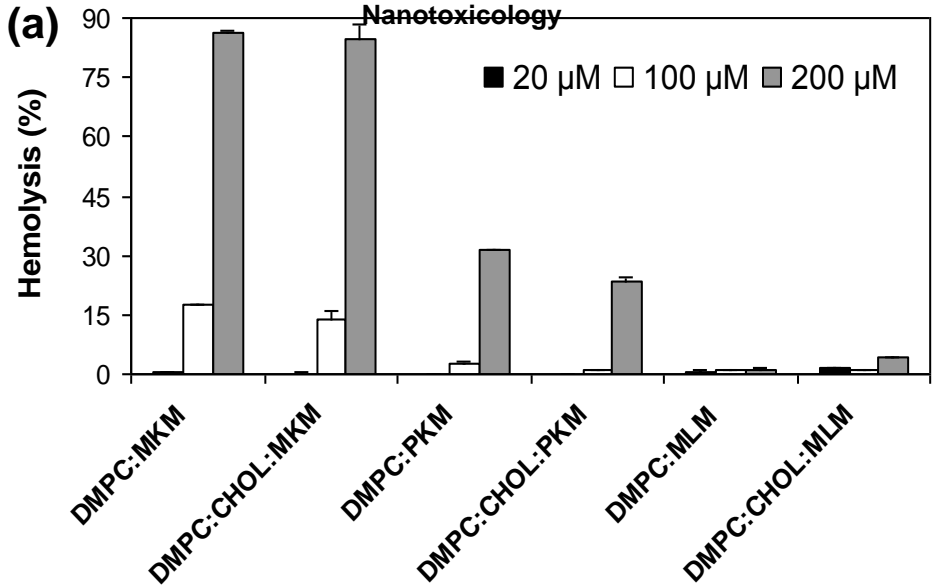
1
2
3
4
5
6
7
8
9
10
11
12
13
14
15
16
17
18
19
20
21
22
23
24
25
26
27
28
29
30
31
32
33





9
10
11
12
13
14
15
16
17
18
19
20
21
22
23
24
25
26
27
28
29
30
31
32
33





1
2
3
4
5
6
7
8
9
10
11
12
13
14
15
16
17
18
19
20
21
22
23
24
25
26
27
28
29
30
31
32
33
34
35
36
37
38
39
40
41
42
43
44
45
46
47
48
49
50
51
52
53
54
55
56
57

1
2
3
4
5
6
7
8
9
10
11
12
13
14
15
16
17
18
19
20
21
22
23
24
25
26
27
28
29
30
31
32
33
34
35
36
37
38
39
40
41
42
43
44
45
46
47
48
49

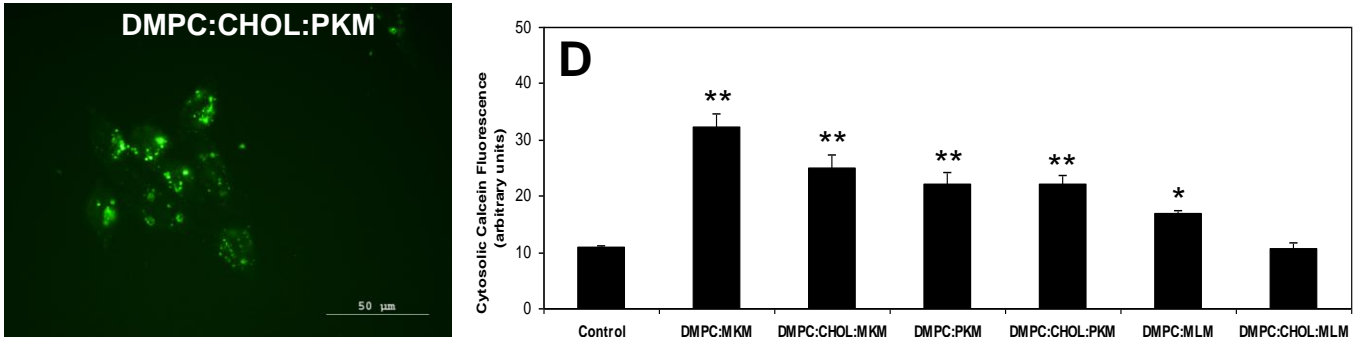
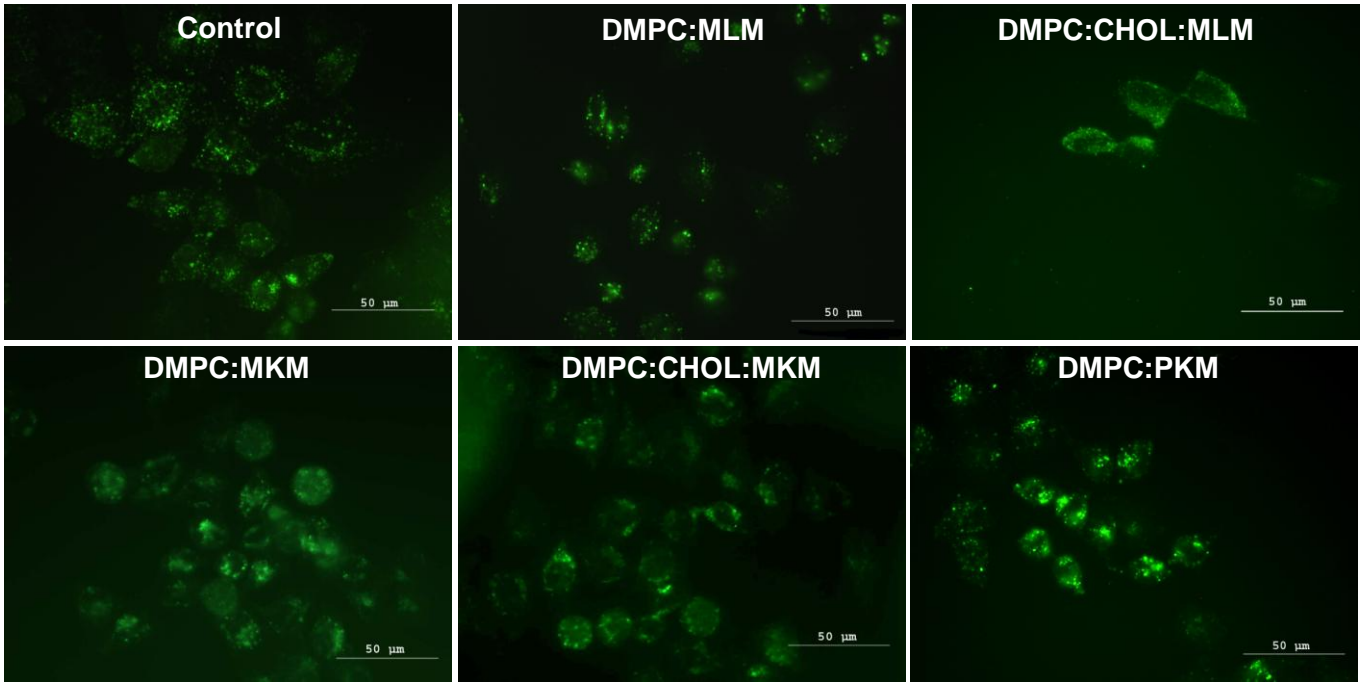
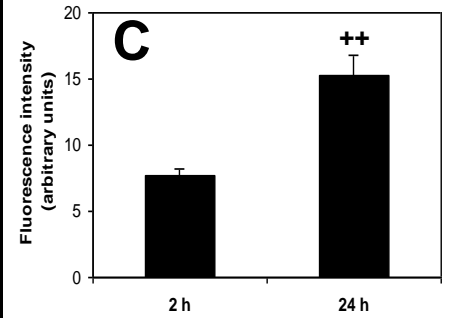
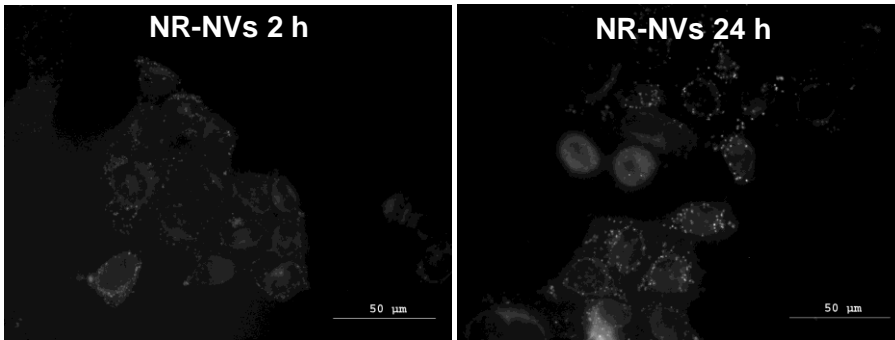
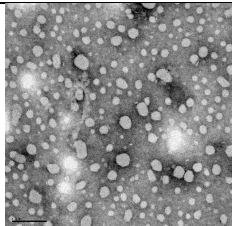
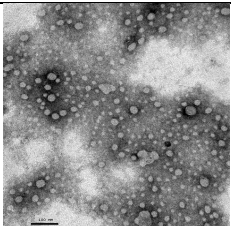
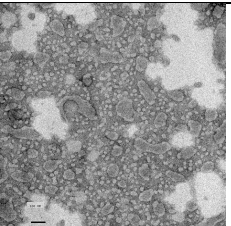
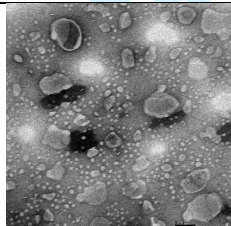
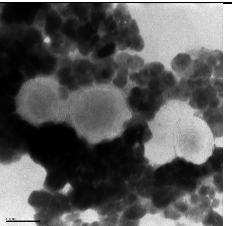



Table 1. Scheme of the nanovesicles' composition.

Nanovesicles	Molar composition (%)		
	DMPC	COLESTEROL (CHOL)	Surfactant (MKM, PKM o MLM)
DMPC:surfactant	80	-	20
DMPC:CHOL:surfactant	56	24	20

For Peer Review Only

Table 2. Characterization properties of the cationic nanovesicles. Values are reported as mean of three independent experiments \pm SEM.

	DMPC:MKM (80:20)	DMPC:CHOL:MKM (56:24:20)	DMPC:PKM (80:20)	DMPC:CHOL:PKM (56:24:20)	DMPC:MLM (80:20)	DMPC:CHOL:MLM (56:24:20)
<i>Size (nm) \pm SEM</i>						
t = 0 h water ^a	94.16 \pm 2.05	107.33 \pm 0.94	253.07 \pm 26.05	184.77 \pm 6.64	174.40 \pm 7.16	127.50 \pm 1.96
t = 0 h DMEM 5% FBS ^a	94.42 \pm 6.50	159.77 \pm 5.71	229.37 \pm 12.64	197.73 \pm 6.57	229.63 \pm 16.33	170.27 \pm 9.49
t = 24 h water ^b	89.39 \pm 3.42	82.59 \pm 5.58	355.6 \pm 31.49/ 68.71 \pm 7.44 ^d	368.47 \pm 19.56/ 77.94 \pm 4.26 ^d	189.53 \pm 5.38	119.57 \pm 4.16
t = 24 h DMEM 5% FBS ^{a,b}	1781.67 \pm 45.72/ 110.3 \pm 5.17 ^d	2028.67 \pm 21.23/ 154.33 \pm 11.95 ^d	1059.50 \pm 10.61/ 118.93 \pm 2.09 ^d	1488 \pm 19.59/ 125.67 \pm 11.94 ^d	193.47 \pm 7.75	151.77 \pm 4.44
t = 1 week water ^c	78.41 \pm 4.76	102.86 \pm 4.19	277.9 \pm 22.16	349.23 \pm 18.45/ 78.64 \pm 4.10 ^d	173.27 \pm 8.19	130.70 \pm 3.20
<i>PDI \pm SEM</i>						
t = 0 h water ^a	0.231 \pm 0.004	0.278 \pm 0.019	0.427 \pm 0.017	0.331 \pm 0.020	0.394 \pm 0.003	0.256 \pm 0.006
t = 0 h DMEM 5% FBS ^a	0.385 \pm 0.015	0.236 \pm 0.001	0.522 \pm 0.001	0.288 \pm 0.001	0.445 \pm 0.007	0.319 \pm 0.029
t = 24 h water ^b	0.371 \pm 0.025	0.378 \pm 0.024	0.508 \pm 0.003	0.523 \pm 0.044	0.399 \pm 0.003	0.239 \pm 0.005
t = 24 h DMEM 5% FBS ^{a,b}	0.903 \pm 0.075	1.00 \pm 0.000	0.605 \pm 0.002	0.973 \pm 0.027	0.294 \pm 0.001	0.352 \pm 0.007
t = 1 week water ^c	0.323 \pm 0.024	0.372 \pm 0.025	0.598 \pm 0.040	0.629 \pm 0.011	0.363 \pm 0.024	0.241 \pm 0.002
<i>Zeta potential (mV) \pm SEM</i>						
t = 0 h water ^a	42.7 \pm 0.90	41.2 \pm 1.66	52.8 \pm 1.15	55.17 \pm 0.67	78.7 \pm 2.56	44.9 \pm 0.40
t = 0 h DMEM 5% FBS ^a	1.23 \pm 1.64	-3.13 \pm 0.81	6.78 \pm 0.94	0.86 \pm 0.11	13.00 \pm 0.49	8.61 \pm 0.16
t = 1 week water ^c	46.67 \pm 1.13	53.97 \pm 1.85	52.23 \pm 0.87	32.15 \pm 2.90	52.53 \pm 0.79	45.90 \pm 1.00
<i>% incorporation of surfactant into NVs \pm SEM ^a</i>						
	88.56 \pm 0.009	75.96 \pm 0.054	99.10 \pm 0.007	98.96 \pm 0.006	90.85 \pm 0.053	79.05 \pm 0.038
<i>TEM diameter (nm) ^e</i>						
t = 0 h water	20 - 50	20 - 50	20 - 50/ 100 - 150	20 - 50/ 100 - 150	150 - 200	90 - 110
TEM images ^{a, f}						

^a Nogueira et al. 2013; ^b Incubated under cell culture conditions: 37°C, 5% CO₂; ^c 4°C; ^d predominant size is indicated first; ^e predominant population; ^f Scale bars = 100 nm;

1
2
3
4
5
6
7
8
9
10
11
12
13
14
15
16
17
18
19
20
21
22
23
24
25
26
27
28
29
30
31
32
33
34
35
36
37
38
39
40
41
42
43
44
45
46
47
48
49

For Peer Review Only

Table 3. Summary of the structure-activity relationship of the cellular events in response to NVs.

	DMPC:MKM	DMPC:CHOL:MKM	DMPC:PKM	DMPC:CHOL:PKM	DMPC:MLM	DMPC:CHOL:MLM
Surfactant charge position	α -amino	α -amino	α -amino	α -amino	ϵ -amino	ϵ -amino
Surfactant alkyl chain length	14C	14C	16C	16C	14C	14C
Surfactant pH-sensitive activity ^a	Yes	Yes	Yes	Yes	No	No
Cytotoxicity by MTT ^b (mitochondrial dysfunction)	++	++	+++	+++	+	+
Cytotoxicity by NRU ^b	+	+	++	+	++	+
Cytotoxicity by LDH ^b	-	-	+	+	+	+
Apoptosis ^c	+	+	+	+	+	+
Cell cycle alteration ^c	-	-	-	-	-	-
Genotoxicity ^c	-	-	+	+	-	-
Oxidative stress ^c	++	+	+++	+	-	+
Endosomal release ^c	+++	+++	+++	+++	++	-
Hemolysis ^c	+	+	+	+	-	-
Erythrocyte agglutination ^c	-	-	-	-	-	-
Plasma protein adsorption ^c	-	-	-	-	-	-

^a As previously reported (Nogueira et al. 2012a, 2012b).

The number of plus signs is a semiquantitative measure according to which: ^b + refers to low ($50 < IC_{50} < 100 \mu M$), ++ to medium ($10 < IC_{50} < 50 \mu M$) and +++ to high cytotoxicity ($IC_{50} < 10 \mu M$). Negligible cytotoxicity was considered when the IC_{50} was higher than $100 \mu M$ (-); ^c + refers to 5-33% value higher than the response of untreated control cells, ++ to 33-66%, and +++ to > 66%. A < 5% value change was considered as equivocal effect (-).

08/03/13

Rightslink Printable License

**ELSEVIER LICENSE
TERMS AND CONDITIONS**

Mar 08, 2013

This is a License Agreement between Pilar Vinardell ("You") and Elsevier ("Elsevier") provided by Copyright Clearance Center ("CCC"). The license consists of your order details, the terms and conditions provided by Elsevier, and the payment terms and conditions.

All payments must be made in full to CCC. For payment instructions, please see information listed at the bottom of this form.

Supplier	Elsevier Limited The Boulevard, Langford Lane Kidlington, Oxford, OX5 1GB, UK
Registered Company Number	1982084
Customer name	Pilar Vinardell
Customer address	Facultat de Farmacia Barcelona, 08028
License number	3104141447408
License date	Mar 08, 2013
Licensed content publisher	Elsevier
Licensed content publication	European Journal of Pharmaceutics and Biopharmaceutics
Licensed content title	New cationic nanovesicular systems containing lysine-based surfactants for topical administration: Toxicity assessment using representative skin cell lines
Licensed content author	Daniele Rubert Nogueira, M. Carmen Morán, Montserrat Mitjans, Verónica Martínez, Lourdes Pérez, M. Pilar Vinardell
Licensed content date	January 2013
Licensed content volume number	83
Licensed content issue number	1
Number of pages	11
Start Page	33
End Page	43
Type of Use	reuse in a journal/magazine
Requestor type	author of new work
Intended publisher of new work	Other
Portion	figures/tables/illustrations
Number of figures/tables/illustrations	1
Format	both print and electronic
Are you the author of this	Yes

<https://s100.copyright.com/AppDispatchServlet>

1/5

08/03/13

Rightslink Printable License

Elsevier article?

Will you be translating? No

Order reference number

Title of the article Lysine-based surfactants in nanovesicle formulations: the role of cationic charge position and hydrophobicity in in vitro cytotoxicity and intracellular delivery

Publication new article is in Nanotoxicology

Publisher of the new article Informa Healthcare

Author of new article Nogueira DR, Morán MC, Mitjans M, Pérez L, Ramos D, Lapuente J, Vinardell MP

Expected publication date Apr 2013

Estimated size of new article (number of pages) 12

Elsevier VAT number GB 494 6272 12

Permissions price 0.00 USD

VAT/Local Sales Tax 0.0 USD / 0.0 GBP

Total 0.00 USD

Terms and Conditions

INTRODUCTION

1. The publisher for this copyrighted material is Elsevier. By clicking "accept" in connection with completing this licensing transaction, you agree that the following terms and conditions apply to this transaction (along with the Billing and Payment terms and conditions established by Copyright Clearance Center, Inc. ("CCC"), at the time that you opened your Rightslink account and that are available at any time at <http://myaccount.copyright.com>).

GENERAL TERMS

2. Elsevier hereby grants you permission to reproduce the aforementioned material subject to the terms and conditions indicated.

3. Acknowledgement: If any part of the material to be used (for example, figures) has appeared in our publication with credit or acknowledgement to another source, permission must also be sought from that source. If such permission is not obtained then that material may not be included in your publication/copies. Suitable acknowledgement to the source must be made, either as a footnote or in a reference list at the end of your publication, as follows:

“Reprinted from Publication title, Vol /edition number, Author(s), Title of article / title of chapter, Pages No., Copyright (Year), with permission from Elsevier [OR APPLICABLE SOCIETY COPYRIGHT OWNER].” Also Lancet special credit - “Reprinted from The Lancet, Vol. number, Author(s), Title of article, Pages No., Copyright (Year), with permission from Elsevier.”

4. Reproduction of this material is confined to the purpose and/or media for which permission is hereby given.

5. Altering/Modifying Material: Not Permitted. However figures and illustrations may be altered/adapted minimally to serve your work. Any other abbreviations, additions, deletions and/or any other alterations shall be made only with prior written authorization of Elsevier Ltd. (Please

<https://s100.copyright.com/AppDispatchServlet>

2/5

08/03/13

Rightslink Printable License

contact Elsevier at permissions@elsevier.com)

6. If the permission fee for the requested use of our material is waived in this instance, please be advised that your future requests for Elsevier materials may attract a fee.

7. Reservation of Rights: Publisher reserves all rights not specifically granted in the combination of (i) the license details provided by you and accepted in the course of this licensing transaction, (ii) these terms and conditions and (iii) CCC's Billing and Payment terms and conditions.

8. License Contingent Upon Payment: While you may exercise the rights licensed immediately upon issuance of the license at the end of the licensing process for the transaction, provided that you have disclosed complete and accurate details of your proposed use, no license is finally effective unless and until full payment is received from you (either by publisher or by CCC) as provided in CCC's Billing and Payment terms and conditions. If full payment is not received on a timely basis, then any license preliminarily granted shall be deemed automatically revoked and shall be void as if never granted. Further, in the event that you breach any of these terms and conditions or any of CCC's Billing and Payment terms and conditions, the license is automatically revoked and shall be void as if never granted. Use of materials as described in a revoked license, as well as any use of the materials beyond the scope of an unrevoked license, may constitute copyright infringement and publisher reserves the right to take any and all action to protect its copyright in the materials.

9. Warranties: Publisher makes no representations or warranties with respect to the licensed material.

10. Indemnity: You hereby indemnify and agree to hold harmless publisher and CCC, and their respective officers, directors, employees and agents, from and against any and all claims arising out of your use of the licensed material other than as specifically authorized pursuant to this license.

11. No Transfer of License: This license is personal to you and may not be sublicensed, assigned, or transferred by you to any other person without publisher's written permission.

12. No Amendment Except in Writing: This license may not be amended except in a writing signed by both parties (or, in the case of publisher, by CCC on publisher's behalf).

13. Objection to Contrary Terms: Publisher hereby objects to any terms contained in any purchase order, acknowledgment, check endorsement or other writing prepared by you, which terms are inconsistent with these terms and conditions or CCC's Billing and Payment terms and conditions. These terms and conditions, together with CCC's Billing and Payment terms and conditions (which are incorporated herein), comprise the entire agreement between you and publisher (and CCC) concerning this licensing transaction. In the event of any conflict between your obligations established by these terms and conditions and those established by CCC's Billing and Payment terms and conditions, these terms and conditions shall control.

14. Revocation: Elsevier or Copyright Clearance Center may deny the permissions described in this License at their sole discretion, for any reason or no reason, with a full refund payable to you. Notice of such denial will be made using the contact information provided by you. Failure to receive such notice will not alter or invalidate the denial. In no event will Elsevier or Copyright Clearance Center be responsible or liable for any costs, expenses or damage incurred by you as a result of a denial of your permission request, other than a refund of the amount(s) paid by you to Elsevier and/or Copyright Clearance Center for denied permissions.

<https://s100.copyright.com/AppDispatchServlet>

3/5

08/03/13

Rightslink Printable License

LIMITED LICENSE

The following terms and conditions apply only to specific license types:

15. **Translation:** This permission is granted for non-exclusive world **English** rights only unless your license was granted for translation rights. If you licensed translation rights you may only translate this content into the languages you requested. A professional translator must perform all translations and reproduce the content word for word preserving the integrity of the article. If this license is to re-use 1 or 2 figures then permission is granted for non-exclusive world rights in all languages.

16. **Website:** The following terms and conditions apply to electronic reserve and author websites:
Electronic reserve: If licensed material is to be posted to website, the web site is to be password-protected and made available only to bona fide students registered on a relevant course if:

This license was made in connection with a course,

This permission is granted for 1 year only. You may obtain a license for future website posting. All content posted to the web site must maintain the copyright information line on the bottom of each image,

A hyper-text must be included to the Homepage of the journal from which you are licensing at <http://www.sciencedirect.com/science/journal/xxxxx> or the Elsevier homepage for books at <http://www.elsevier.com>, and

Central Storage: This license does not include permission for a scanned version of the material to be stored in a central repository such as that provided by Heron/XanEdu.

17. **Author website** for journals with the following additional clauses:

All content posted to the web site must maintain the copyright information line on the bottom of each image, and the permission granted is limited to the personal version of your paper. You are not allowed to download and post the published electronic version of your article (whether PDF or HTML, proof or final version), nor may you scan the printed edition to create an electronic version. A hyper-text must be included to the Homepage of the journal from which you are licensing at <http://www.sciencedirect.com/science/journal/xxxxx>. As part of our normal production process, you will receive an e-mail notice when your article appears on Elsevier's online service ScienceDirect (www.sciencedirect.com). That e-mail will include the article's Digital Object Identifier (DOI). This number provides the electronic link to the published article and should be included in the posting of your personal version. We ask that you wait until you receive this e-mail and have the DOI to do any posting.

Central Storage: This license does not include permission for a scanned version of the material to be stored in a central repository such as that provided by Heron/XanEdu.

18. **Author website** for books with the following additional clauses:

Authors are permitted to place a brief summary of their work online only.

A hyper-text must be included to the Elsevier homepage at <http://www.elsevier.com>. All content posted to the web site must maintain the copyright information line on the bottom of each image.

You are not allowed to download and post the published electronic version of your chapter, nor may you scan the printed edition to create an electronic version.

Central Storage: This license does not include permission for a scanned version of the material to

<https://s100.copyright.com/AppDispatchServlet>

4/5

08/03/13

Rightslink Printable License

be stored in a central repository such as that provided by Heron/XanEdu.

19. **Website** (regular and for author): A hyper-text must be included to the Homepage of the journal from which you are licensing at <http://www.sciencedirect.com/science/journal/xxxxx> or for books to the Elsevier homepage at <http://www.elsevier.com>

20. **Thesis/Dissertation**: If your license is for use in a thesis/dissertation your thesis may be submitted to your institution in either print or electronic form. Should your thesis be published commercially, please reapply for permission. These requirements include permission for the Library and Archives of Canada to supply single copies, on demand, of the complete thesis and include permission for UMI to supply single copies, on demand, of the complete thesis. Should your thesis be published commercially, please reapply for permission.

21. **Other Conditions**:

v1.6

If you would like to pay for this license now, please remit this license along with your payment made payable to "COPYRIGHT CLEARANCE CENTER" otherwise you will be invoiced within 48 hours of the license date. Payment should be in the form of a check or money order referencing your account number and this invoice number RLNK500972980. Once you receive your invoice for this order, you may pay your invoice by credit card. Please follow instructions provided at that time.

**Make Payment To:
Copyright Clearance Center
Dept 001
P.O. Box 843006
Boston, MA 02284-3006**

For suggestions or comments regarding this order, contact RightsLink Customer Support: customercare@copyright.com or +1-877-622-5543 (toll free in the US) or +1-978-646-2777.

Gratis licenses (referencing \$0 in the Total field) are free. Please retain this printable license for your reference. No payment is required.

<https://s100.copyright.com/AppDispatchServlet>

5/5